AD-A031 534 SCOPE ELECTRONICS INC RESTON VA F/G 17/1
EVALUATION OF CONFLEX I CAPABILITIES IN CLASSIFYING SONAR CONTA--ETC(U)
NOV 65 NOBSR-91208

UNCLASSIFIED NL

1 OF 1
AD
A031534

END
DATE
FILMED
12-76

14,500-c

[redacted] UNCLASSIFIED

Copy No. 1 of __ Copies

(9)

FINAL REPORT

(6)

EVALUATION OF CONFLEX I CAPABILITIES
IN
CLASSIFYING SONAR CONTACTS

BUREAU OF SHIPS CONTRACT NOBSR-91208 new
PROJECT SERIAL NO. SF0070101, TASK 7131

(15)

Prepared by:

(12) 59p.

SCOPE INCORPORATED
2816 FALLFAX DRIVE
FALLS CHURCH, VIRGINIA 22042

(11)

5 NOVEMBER 1965

DDC
RECEIVED
NOV 2 1976
A

DISTRIBUTION STATEMENT A
Approved for public release;
Distribution Unlimited

NOTICE

This material contains information affecting the national defense of the United States within the meaning of the Espionage laws, Title 18, U.S.C., Sections 793 and 794. The transmission or revelation of this information in any manner to an unauthorized person is prohibited by law.

318 650
bpg

Downgraded at 3 Year Intervals
Declassified after 12 Years
DOD DIR 5200.10

UNCLASSIFIED

[redacted]

14,500-c

14,500-c

[redacted] UNCLASSIFIED

ABSTRACT

The results of a number of pattern recognition experiments designed to evaluate the performance of the CONFLEX I system in classifying sonar contacts are reported. CONFLEX I is a laboratory experimental pattern-recognition system developed under Air Force contract. Theoretical measures of system performance are reviewed as background for the experiment evaluations.

Utilizing a series of specially formatted photographic transparencies representing 132 submarine and 73 nonsubmarine returns, three major experiments were run on the CONFLEX I system: A closed-ended experiment to test the system's ability to separate two classes; an open-ended experiment to measure the system's ability to categorize inputs which were not used in training; a test of the system's performance when subdividing the submarine returns into aspect groups.

Classifications in these experiments were 94.1%, 85.9% and 97.6% correct, respectively. Distribution plots, "ROC" curves, and computed probabilities of correct response are included in the experiment evaluations.

Signal preprocessing and slide preparation were greatly aided by the computing facilities and personnel of the Applied Mathematics Laboratory of the David Taylor Model Basin.

UNCLASSIFIED
[redacted]

TABLE OF CONTENTS

ILLUSTRATIONS

INTRODUCTION

Acoustic signals received by active sonar equipment have for years been a major source of underwater threat information for the human classifier. A number of interesting techniques for acquiring and processing target information have been investigated, but classification concepts utilizing information derived from the sonar return continue to offer the greatest promise.

Automatic, rapid, and accurate classification of sonar contacts in the underwater environment is an urgent ASW requirement and is the focus of current research. An extensive effort is being made to develop a data processor in which the advanced capabilities (e.g., greater source levels and mode and signal flexibility) of the newer sonar equipment are exploited. Satisfactory achievement of this objective has proven unusually difficult.

This final report presents the results of classification experiments which, although necessarily limited, were designed to evaluate the capability of a pattern-recognition system, CONFLEX I, to distinguish submarine from nonsubmarine sonar returns. CONFLEX I is a unique pattern-recognition system that implements a concept referred to as "conditioned-reflex." Such a system is "conditioned" by allowing the processor to derive and store in its memory a reference function for a given set of multivariable input patterns or stimuli. The

"response" to an unknown input, which is similarly processed, is to associate the input with the set whose reference function shows the greatest cross-correlation. The concept has proven exceptionally effective in various pattern-recognition problems, many of which are similar to those encountered in sonar return classification.

The experiments performed under this study contract could not, within the limitations of the contract, be expected to be conclusive. Nevertheless, we were encouraged by the results* of those experiments which we were able to perform. Section I reviews important aspects of the conditioned-reflex concept. Much of this material has been presented previously in documents generated by SCOPE but is included in this report as reference for the system performance evaluation and as background for those not familiar with our work. A complete treatment is contained in reference 1. We begin with a description of the CONFLEX I system; however, readers familiar with the system can proceed directly to section II.

---

* These results are reported in section IV.

SECTION I

SUMMARY, CONDITIONED-REFLEX THEORY AND ITS IMPLEMENTATION IN CONFLEX I

CONFLEX I, shown in figure 1, has been designed for laboratory experiments in pattern recognition. This system consists of an optical input (receptor) device and a digital data processor that transforms the input data, utilizing cross-correlation decision criteria. In the present configuration of the CONFLEX, inputs are presented to the receptor by projecting 35 mm slides onto an array of photo-resistors. This method of presenting data has proven useful in a wide range of experimentations, but, of course, is not the type one would design in a system for processing transient signals such as those encountered in the sonar environment. Nevertheless, the method is often expedient in attempts to evaluate the applicability of the CONFLEX concept during preliminary explorations of a new problem. Such was the case in this study program. As a matter of interest, the work reported herein was the forerunner of a larger-scale program, with similar objectives, which is now in progress. In this program, many thousands of examples will be processed utilizing a more efficient buffer between the magnetic tape records and the CONFLEX system.

The mode of operation in CONFLEX I is sequential but efficient for most laboratory experiments. System logic is implemented with one-megacycle plug-in module cards, and the memory

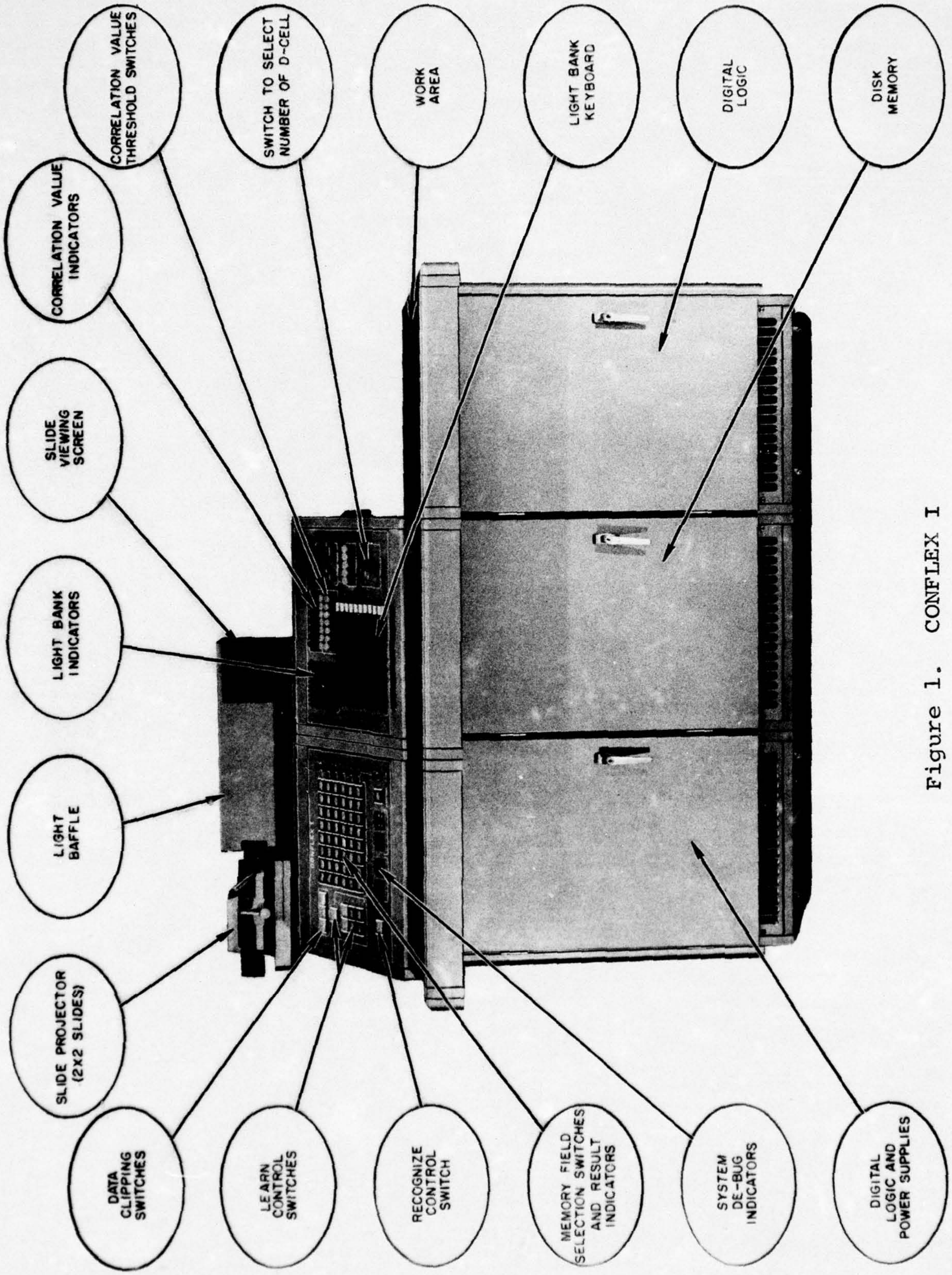

Figure 1. CONFLEX I

is a 500,000 bit magnetic disc. All clock and timing information is derived from the memory disc. In CONFLEX I, the clock rate is about 300 kc (corresponding to 60 rps and 5100 bits/revolution).

LABORATORY MODEL OPERATIONS

In the laboratory model, information is extracted from input patterns sequentially by means of a linear threshold circuit (the D-cell). Connected to this circuit during each clock interval is a unique random sample of outputs from the sensory system. The particular random connections depend on the states of several linear feedback shift registers. As these shift registers are strobed by the system clock, random, but repeatable, connections are made at the rate of thirty million per second. The resulting sequence of D-cell outputs characterizes the input signal.

In the LEARN, or adaptive, phase of system operation, the D-cell sequences are combined by the data processor to form a reference sequence associated with each pattern class. The assignment of inputs to a class and storage of references are under operator control during the LEARN phase.

CONFLEX I automatically classifies an "unknown" input in the RECOGNIZE phase of system operation. The decision function is based upon a cross-correlation between the D-cell sequence for the unknown and each of the stored reference sequences. Class assignment of the unknown normally corresponds to the

reference yielding the highest positive correlation. Correlation values can be compared with a fixed threshold in an alternative mode of operation.

Depending on the mode of reference storage, 6, 24, or 48 classes are available, and correlations are performed in about 16.5 msec per class. Hence, about 3/4 second is required to choose from among 48 classes the assignment of an unknown.

DATA PROCESSOR OPERATIONS

Given a set of possible inputs, together with a specified class assignment for each, the data processor derives and stores data later used to automatically decide the class of an unknown input. The basic decision process consists of comparing the data derived from the unknown input with the stored data for each class. Expected inputs are generally represented by a relatively large number of sample points.

In the conditioned-reflex processor (CR System), the decision function is implemented by cross-correlation. Stored within the system is reference data corresponding to each class. The manner in which data is derived from the inputs and combined to form the references is such as to make cross-correlation highly efficient for a large number of anticipated recognition problems.

BASIC ORGANIZATION OF THE CR SYSTEM

Figure 2 is a block diagram of the basic organization of the conditioned-reflex system. Since CONFLEX I has an optical

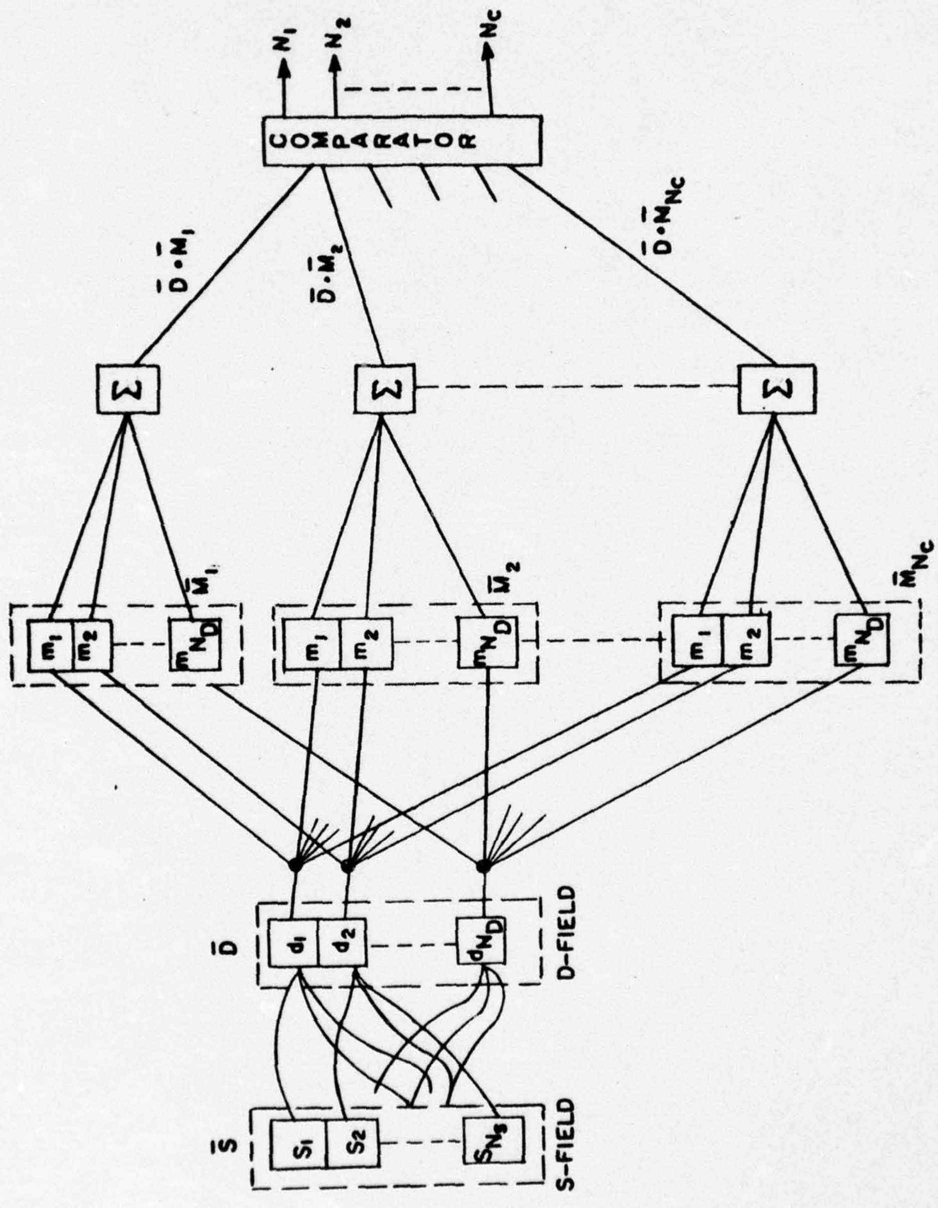

Figure 2. Conditioned-Reflex Organization

receptor, we will discuss the model in terms of visual input patterns (stimuli). The stimuli are placed on a two-dimensional field (the sensory field), subdivided into N_S sensory resolution cells (S-cells). A stimulus may be represented by a vector, $\bar{S}_j$, in a space of N_S dimensions, where the value of each component depends upon the light intensity on the corresponding S-cell. For a white-black pattern, these components may be taken as unity or zero.

The sensory field (S-field) is connected to a second field called the discrimination field (D-field). These connections are made in such a way that vector $\bar{S}_j$ is transformed into a new vector, $\bar{D}_k$, with N_D elementary components. Each component has a value determined by the output of the corresponding discrimination cell (D-cell). For example, this output d_k could be +1, 0, or -1 when the algebraic sum of its several inputs is greater than zero, equal to zero, or less than zero, respectively. In this case, we refer to a simple linear threshold logic. Other D-field logics are generally used, yielding superior experimental results.

A D-cell receives a random selection of inputs from the S-field. This method of connection makes two D-field responses substantially different (as measured by a comparison of the corresponding D-cell outputs) even when the stimuli are similar. It is this property of the system that allows reliable separation of similar inputs. The intended response of the system when a stimulus is applied is to select the appropriate one of a set of N_C responses $\left(R_1, R_2, \ldots, R_{N_C}\right)$. The choice of class assignment,

C_j (therefore, response R_j), involves the correlation of the linear threshold measurements made on the unknown pattern by the D-cells, with each of a number of reference functions stored in the memory fields (M-fields). These references can be visualized as a set of vectors (M-vectors) in a multidimensional space or, alternatively, as a set of planes through its origin. The set of linear threshold measurements, d_{ki}, made upon each input are the components of the vector $\bar{D}_k$ drawn from the origin of the space to the point having coordinates $\left(d_{k1}, d_{k2}, \ldots, d_{kN_D}\right)$.

Each reference vector is formed by adding vectorially the D-vectors corresponding to the set of inputs to be classified together. The components of M-vector $\bar{M}_j$ are therefore given by

$$\bar{M}_j = \left(m_{j1}, m_{j2}, \ldots, m_{jN_D}\right), \tag{1}$$

where $$m_{ji} = \sum_{k=1}^{N_E} d_{ki} \qquad \text{and} \qquad i = 1, 2, \ldots, N_D.$$

In this example, N_E input patterns are used to construct the j^{th} reference function. Note that for each reference there is one m_{ji} corresponding to each D-cell d_{ki}.

Figure 3 shows a simple example in only three dimensions; i.e., $N_D = 3$. The general equation for a plane through the origin is given by $ax_1 + bx_2 + cx_3 = 0$. When the coefficients, a, b, c, are replaced by the coordinates of $\bar{M}$, the resulting plane is perpendicular to $\bar{M}$; that is, $\bar{M}$ is normal to the plane.

$$m_1x_1 + m_2x_2 + m_3x_3 = 0. \tag{2}$$

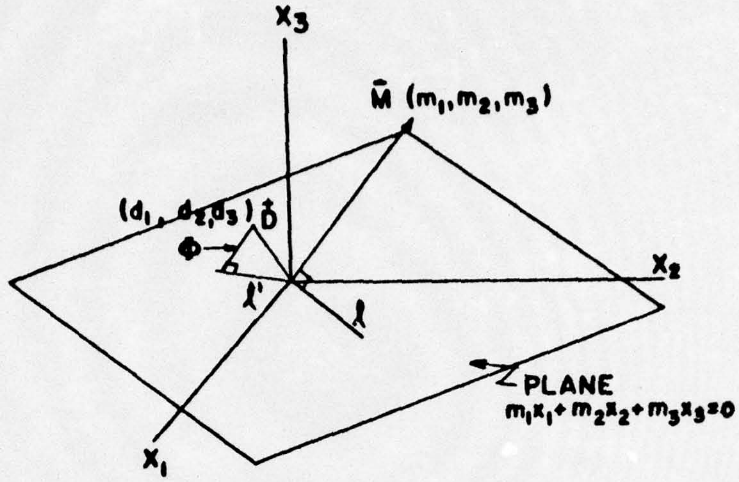

Figure 3. Geometrical Interpretation of Classification Criterion

The correlation of an input with the j^{th} reference is given by

$$\Phi_{xj} = \bar{D}_x \cdot \bar{M}_j = \sum_{i=1}^{N_D} d_{xi} m_{ji}. \tag{3}$$

$\bar{D}_x \cdot \bar{M}_j$ is a vector dot product. This is equivalent to replacing the x_i's with the d_{xi}'s in equation 2. In the three-dimensional system,

$$\Phi = m_1 d_1 + m_2 d_2 + m_3 d_3. \tag{4}$$

Except for a normalizing factor $\sqrt{m_1^2 + m_2^2 + m_3^2}$, this is the distance from the point (d_1, d_2, d_3) to the plane defined by equation 2. In the CR System, the unknown may be associated with the reference yielding the largest Φ. It is therefore assigned by the comparator (figure 2) to class C_j when the

reference, whose vector $\bar{M}_j$ is closest to $\bar{D}_x$ or, alternatively, whose plane $0 = \sum_{i=1}^{N_D} m_{ji} x_i$ is farthest from the point $\left(d_{x1}, d_{x2}, \ldots, d_{xN_D}\right)$.

A two-class decision problem using vector notation is illustrated in figure 4. In this example the unknown, represented by $\bar{D}_x$, would be associated with class 2. Note that the plane (equation 2) is optimum with respect to the point $\left(m_1, m_2, m_3\right)$ in the sense that no other plane can be drawn through the origin and be as far from the point. However, the plane may not be optimum with respect to a point $\left(d_1, d_2, d_3\right)$; for this reason, incorrect class assignment is possible.

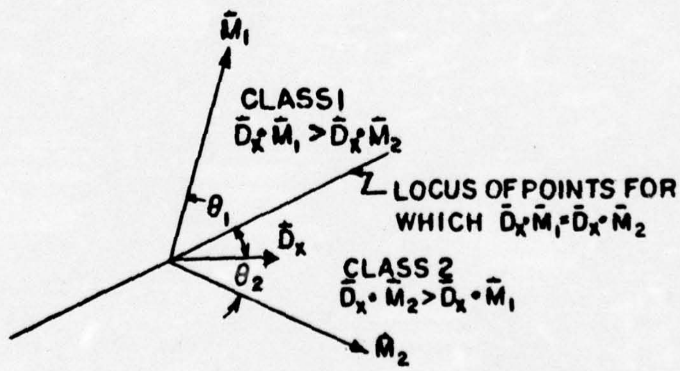

Figure 4. Two-class Decision Problem

REVIEW OF IMPORTANT ANALYTICAL RESULTS

The decision process has been described as one of calculating the several values of the vector dot products given by $\bar{D}_x \cdot \bar{M}_j$ and associating the unknown input with the class whose M-vector yields the largest dot product. $\bar{D}_x$ is the D-vector generated by the system for the unknown $\bar{S}_x$. There are two cases of interest: first, $\bar{D}_x \cdot \bar{M}_j$, where $\bar{S}_x$ is not in class C_j $\left(\text{i.e., } \bar{D}_x \notin \bar{M}_j\right)$; second, $\bar{D}_x \cdot \bar{M}_j$, where $\bar{S}_x$ is a member of C_j $\left(\text{i.e., } \bar{D}_x \in \bar{M}_j\right)$. The first case is associated with the noise in the decision process, and the second is identified with the signal. The dot products are random variables, the values of which are the possible results of computing $\bar{D}_x \cdot \bar{M}_j$ for a large ensemble of machines identically conditioned and organized according to the same probabilistic specification.

Probability of Correct Response

Figure 2 shows the several dot products entering the comparator. Let S be the actual value of comparator input containing the signal; that is, $S = \bar{D}_x \cdot \bar{M}_j$, where $\bar{D}_x$ is one of the D-vectors originally used to construct $\bar{M}_j$. The response will be correct only if none of the N_C-1 other inputs to the comparator exceeds S. If each of the other inputs has mean μ_N and variance σ_N^2, the probability of the joint event that none of the other inputs should exceed S is

$$P(S) = \left[\frac{1}{\sigma_N\sqrt{2\pi}} \int_{-\infty}^{S} \exp - \frac{\left(x-\mu_N\right)^2}{2\sigma_N^2}\, dx\right]^{N_C-1} ; \qquad (5)$$

provided the comparator inputs can be described by statistically independent Gaussian processes.

For S, a normally distributed random variable with mean μ_S and variance σ_S^2, the probability of correct response is derived by averaging P(S) over S as follows:

$$P_c = \frac{1}{\sigma_S\sqrt{2\pi}} \int_{-\infty}^{+\infty} P(S) \exp - \frac{\left(S-\mu_S\right)^2}{2\sigma_S^2} \, dS. \qquad (6)$$

We would like to have an expression that is more easily evaluated for various values of μ and σ. To obtain an underestimate of P_c, we replace S by its mean value, μ_S, and augment the variance of the N_c-1 other inputs to the comparator by the variance of S. Then each of the other inputs has variance $\sigma_T^2 = \sigma_S^2 + \sigma_N^2$, but the N_c-1 new random variables are no longer independent. Neglecting this fact (the resulting error is conservative), the joint probability that none of the other inputs exceeds μ_S is

$$P_c' = \left[\frac{1}{\sigma_T\sqrt{2\pi}} \int_{-\infty}^{\mu_S} \exp - \frac{\left(x-\mu_N\right)^2}{2\sigma_T^2} \, dx \right]^{N_c-1} . \qquad (7)$$

Changing variables by letting $y = \frac{x-\mu_N}{\sigma_T}$ transforms P_c' into normal form

$$P_c' = \left[\frac{1}{\sqrt{2\pi}} \int_{-\infty}^{\Gamma} \exp - \frac{y^2}{2} \, dy \right]^{N_c-1} , \qquad (8)$$

where $\Gamma = \frac{\mu_S - \mu_N}{\sigma_T}$. The probability of correct response therefore becomes a tabulated function of Γ. Values of P'_c as a function of Γ can be found in most mathematics handbooks and in texts on probability and statistics (references 2 and 3). An abbreviated table is included here as an appendix.

Hereafter, Γ will be referred to as the signal-to-noise ratio. It is used extensively in reference 1 for comparison of variations of the CR model. In the following paragraphs, Γ is computed for two cases of special interest. It is used in section IV to evaluate experimental results.

Unclipped Reference Vectors

Unclipped reference vectors $\bar{M}_j$ are constructed by vector addition of the D-vectors corresponding to the training stimuli assigned to class C_j. Each $\bar{M}_j$ is therefore given by

$$\bar{M}_j = \bar{D}_{j1} + \bar{D}_{j2} + \cdots + \bar{D}_{jN_E} \quad \text{(vector sum)}, \tag{9}$$

where N_E is the number of stimuli used in forming the class reference. Since equation 9 is vector addition, the i^{th} component of $\bar{M}_j$ is written

$$m_{ji} = d_{j1i} + d_{j2i} + \cdots + d_{jN_E i}. \tag{10}$$

In order to compute Γ, one investigates the mean and variance of the dot products $\bar{D}_x \cdot \bar{M}_j$ for each of the noise and signal cases. Hence, the statistics of the products $d_{jxi} m_{ji}$ are required. It is shown in reference 1 that for a CR system in which

the D-cell outputs are uncorrelated, random variables with zero means that the signal-to-noise ratio is

$$\Gamma^2 = \frac{N_D}{2N_E} \quad \text{(unclipped reference vectors).} \tag{11}$$

It is also shown that equation 11 holds when a majority decision is made such that a D-cell output is +1 when the sum of its inputs is positive, -1 when the sum is negative, and zero otherwise.

Our estimate of the probability of correct response P_C' (equation 8) is

$$P_C' = (0.9987)^{N_C - 1} \tag{12}$$

for $\Gamma = 3$. Of particular importance to the design of the CR system is the number of D-cells, N_D. Equation 11 can be used to determine the required N_D for a given Γ and number of stimuli per class, N_E. Hence, for example, if $\Gamma = 3$ and $N_E = 100$, we have $N_D = 1800$. For $N_C = 20$, our estimate gives $P_C' = 0.9756$; that is, on the average, about 50 of the 2000 stimuli used to condition the system would be misclassified.

In a digital system, the number of bits of storage required for the reference vectors in the unclipped case is equal to $N_C N_D \log_2(2N_E)$. A method for substantially reducing this requirement relates to a "clipped system," described next.

Clipped Reference Vectors

The components m_{ji} of the reference vectors in the unclipped system are random variables taking on integral values in the range

$$-N_E \leq m_{ji} \leq +N_E. \tag{13}$$

In the clipped system, these components are replaced by binary variables $\dot{m}_{ji}$ having integral values either +1 or -1. The clipping operation is such that $\dot{m}_{ji} = +1$ when $m_{ji} \geq 0$, and $\dot{m}_{ji} = -1$ when $m_{ji} < 0$. It should be emphasized that this operation takes place only after the corresponding unclipped reference vector has been formed.

The signal-to-noise ratio for this clipped system is

$$\Gamma^2 = \frac{N_D}{\pi N_E} \quad \text{(clipped reference vectors)}. \tag{14}$$

Using the same numbers as in the previous example (i.e., N_D = 1800; N_E = 100), the signal-to-noise ratio for this case becomes Γ = 2.4. The probability of correct response (again for N_C = 20) is P_c' = 0.8550. About 290 of the 2000 trained stimuli would be misclassified.

It is instructive to compute the number of D-cells required in the clipped system to yield Γ = 3 (therefore, the same P_c' as in the unclipped example), then, to compare the required binary storage for the two systems:

$$N_D \text{ (clipped)} = 2826 \tag{15}$$

In general, N_D (clipped) = $\frac{\pi}{2}$ N_D (unclipped). Since the number of bits of storage required for the clipped system is equal simply to $N_D N_C$, the two systems compare on an equal P'_c basis as follows:

$$\frac{\text{(required storage clipped)}}{\text{(required storage unclipped)}} = \frac{N_C \frac{\pi}{2} N_D}{N_C N_D \log_2 2N_E}$$

$$= \frac{\pi}{2\log_2 2N_E} \qquad (16)$$

For N_E = 100, the clipped system required about 23 percent as much as is used by the unclipped model.

This economy of storage is used to good advantage in CONFLEX I. In this system, six classes of unclipped storage are replaced by 48 classes in the clipped operating mode.

Replacement of Comparator by a Fixed Threshold

The comparator illustrated in figure 2 compares the N_C correlations $\bar{D}_x \cdot \bar{M}_j$ and selects the response corresponding to the memory vector producing the greatest positive correlation. An alternative mode (implemented in CONFLEX I) is that in which the correlations are compared with a fixed threshold, T. The rule for this mode of operation is that the response R_k is made if $\bar{D}_x \cdot \bar{M}_k \geq T$.

In such a system, it is clearly possible to produce two or more simultaneous responses, a situation repeatedly encountered in statistical-decision theory. Two types of errors must

be considered. The first is that of failure to produce a response when, in fact, $\bar{D}_x$ is contained in $\bar{M}_j$. The probability of this error is

$$P_1 = \frac{1}{\sigma_S\sqrt{2\pi}} \int_{-\infty}^{T} \exp - \frac{\left(x-\mu_S\right)^2}{2\sigma_S^{\,2}}\, dx \tag{17}$$

The second type of error is that of incorrectly producing one or more responses, R_k, when, in fact, $\bar{D}_x$ is not contained in $\bar{M}_j$. The probability of this error is

$$P_2 = 1 - \left[\frac{1}{\sigma_N\sqrt{2\pi}} \int_{-\infty}^{T} \exp - \frac{x^2}{2\sigma_N^{\,2}}\, dx\right]^{N_C - 1} \tag{18}$$

The probabilities P_1 and P_2 depend upon the threshold T, and the value of T can be chosen in a variety of ways. For example, if losses or penalties are assigned to each type of error, one can ask for the value of T which minimizes the overall expected loss. This is Bayes' criterion.

Alternatively, one may stipulate that, say, the first type of error is to be held below a prescribed level, and within this restriction a value of T is to be chosen which minimizes the second type of error. This is the Neyman-Pearson criterion.

Using a fixed threshold, even with the most favorable choice of T, will require a greater value of N_D to meet a specified

overall error rate. This is an understandable result in view of the added constraint imposed by the fixed threshold. One advantage of using a fixed threshold criterion for response selection is that the response selection logic becomes relatively easy to implement.

SUMMARY OF MODEL PARAMETERS

CONFLEX I can be used as an unclipped or clipped model, and responses can be selected either by the comparator or, if desired, by the fixed-threshold method. It is also possible to "partially clip" the M-vector components in such a way that

$$\dot{m}_{ji} = +1 \text{ when } m_{ji} \geq +\tau$$

$$\dot{m}_{ji} = -1 \text{ when } m_{ji} \leq -\tau$$

$$\dot{m}_{ji} = \ \ 0 \text{ when } -\tau < m_{ji} < +\tau .$$

A discussion of this general clipping mode is found in reference 4.

The number of D-cells implemented in CONFLEX I is variable in steps from 500 to 5000. In the clipped mode, 48 classes are possible, while six are implemented in the unclipped mode. Since two bits per $\dot{m}_{ji}$ are required in partially clipped operation, 24 classes are possible in this mode.

The sensory system in CONFLEX I consists of 400 photoresistors connected in a checkerboard pattern of plus and minus contributors. These will be referred to as excitatory and inhibitory cells, respectively. Reference 1 shows the desirability of having a relatively large number of these cells connected to each D-cell.

EVALUATING SYSTEM PERFORMANCE

Equation 8, which gives the probability of correct response under controlled experimental conditions, is a generally useful expression for estimating system performance. Evaluation of this expression requires that relatively large experiments (i.e., numbers of patterns) be performed to obtain statistically significant data. The appendix tabulates the probability of correct response, P_c', in a two-class ($N_C = 2$) problem for Γ in the range $0.0 \leq \Gamma < 4.0$. The values are plotted in figure 5.

The quantity Γ, which was derived earlier, is repeated here for convenience:

$$\Gamma = \frac{\left(\mu_S - \mu_N\right)}{\sigma_T} \tag{19}$$

where $\mu_S = E\left(\bar{D}\cdot\bar{M}_j\right)$, $\bar{D}$ is contained in $\bar{M}_j$

$\mu_N = E\left(\bar{D}\cdot\bar{M}_k\right)$, $\bar{D}$ is not contained in $\bar{M}_k$;

and $\sigma_T = \sqrt{\sigma_S^2 + \sigma_N^2 - 2\mathrm{cov}\left(\bar{D}\cdot\bar{M}_j,\ \bar{D}\cdot\bar{M}_k\right)}$

where the prefix E is used to denote expected value.

An experimental Γ may be computed by substituting empirical results in the above expression. In the following example of this derivation, correlation values are given for a two-class experiment. Ten images were used in the experiment - five to form each of two classes. The correlation values that resulted from testing each of the ten images with both learned classes are shown.

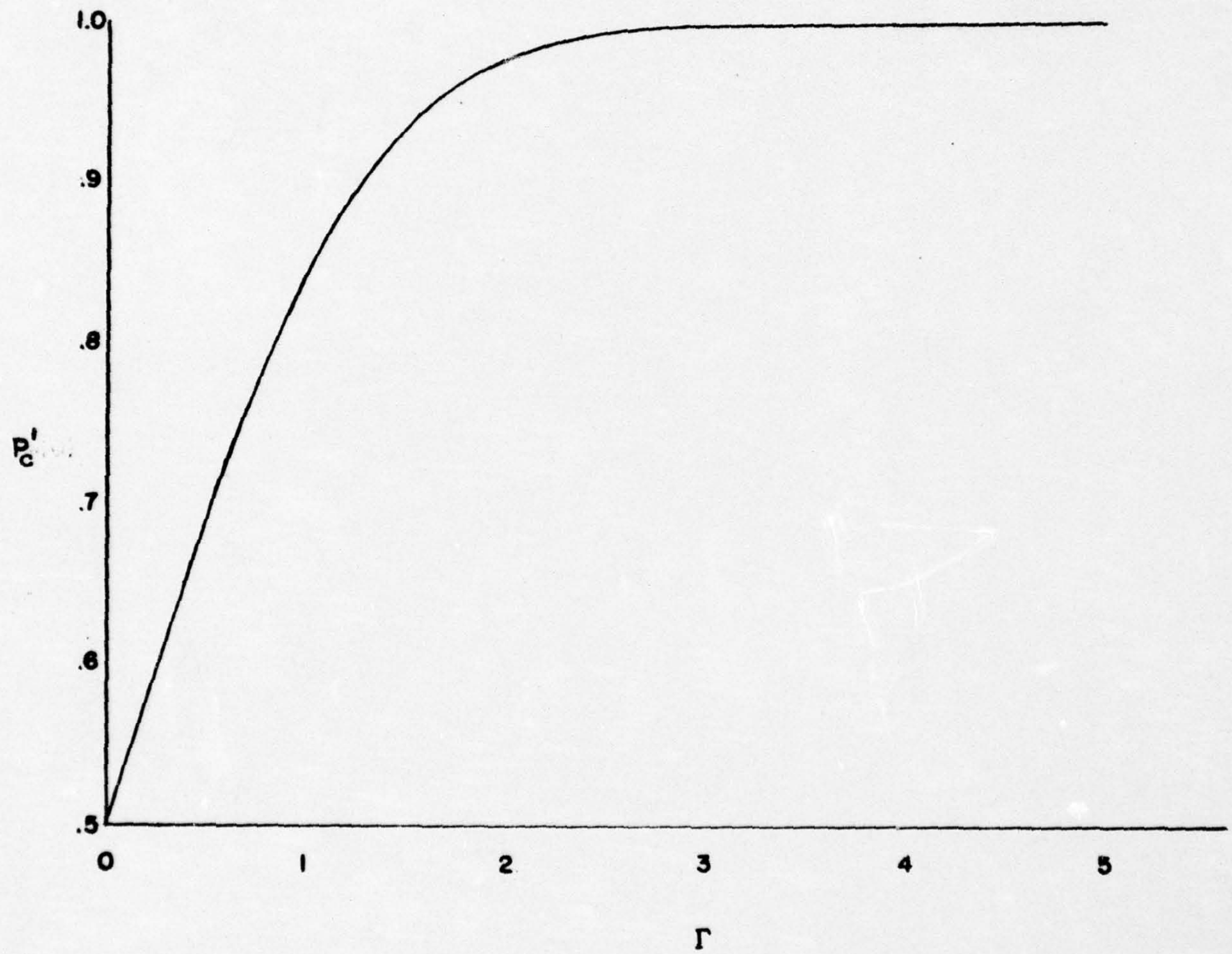

Figure 5. Two-Class Probability of Correct Response as a Function of Γ

Image Number	In-class Signal Values (x_i)	Out-of-class Noise Values (y_i)
1	66	- 5
2	60	22
3	33	- 5
4	80	13
5	57	6
6	66	20
7	57	7
8	44	16
9	62	1
10	41	16

The statistical measures appearing in equation 19 are the mean, μ, variance, standard deviation, σ, and covariance. In evaluating experimental results, we use sample statistics and compute these measures using the following expressions:

$$\text{Mean} = \mu = \frac{1}{n} \sum_{i=1}^{n} x_i \tag{20}$$

$$\text{Variance} = \sigma^2 = \frac{1}{n-1} \sum \left(x_i - \bar{x}\right)^2 \tag{21}$$

$$\text{Covariance} = \frac{1}{n-1} \sum \left(x_i - \bar{x}\right)\left(y_i - \bar{y}\right) \tag{22}$$

where n is the total number of sample results (e.g., ten in the above example).

Using the in-class and out-of-class correlation values listed above, we find that

μ_S = 56.6 = mean of the in-class values

μ_N = 9.1 = mean of the out-of-class values

σ_S^2 = 191.6 = variance of the in-class values

σ_N^2 = 97.0 = variance of the out-of-class values

Cov = 21.9 = covariance of the in-class and out-of-class values

Substituting these values into the expression for Γ,

$$\Gamma = \frac{(\mu_S - \mu_N)}{\sigma_T} = \frac{(\mu_S - \mu_N)}{\sqrt{\sigma_S^2 + \sigma_N^2 - 2\mathrm{Cov}}} = \frac{56.6-9.1}{\sqrt{191.6+97.0-2(21.9)}} = 3.0$$

Referring to the appendix, we observe that a Γ of 3.0 indicates a probability of correct response equal to 0.9987 or an expected error rate of 13 per 10,000 in a two-class experiment.

This example illustrates the relatively high signal-to-noise ratio that results when relatively few D-vectors are used to form each M-vector. Statistically significant error-rate data is obtained by performing hundreds of experiments or, alternatively, performing relatively few experiments but using a very large number of images per class. By computing the experimental Γ, experiments can be designed which are relatively simple and yet

statistically meaningful. Hereinafter, the experimental Γ is used to measure system performance since the expected error rate may be readily determined from either figure 5 or the appendix.

SECTION II

BASIS FOR CLASSIFICATION

In the unrestricted classification problem, one attempts to mechanize mathematical transformations in which all "similar patterns" are mapped into a single representative class symbol. These invariances have long been sought by engineers and mathematicians as a means of obviating complications introduced by variations in patterns; e.g., medium effects, target strength, aspect, etc., related to the sonar. Most of the transformations discovered are useful only with pattern environments of academic interest, while those exhibiting the desired generality have proven unusually complex when they are considered as a basis for machine design.

The design of a classification system begins with the selection of a set of measurements. The measurements are usually selected on the basis of the best available physical knowledge of the problem, but they often include measurements which past experience has shown to be useful. Sonar systems include a number of displays that serve as the primary source of classification information for the experienced operator. The sonarman speaks of echo quality and doppler, echo strength, and echo length when listening to the audio. On his PPI scope he looks for pip shape, intensity, target angle and movement to give him additional clues. From his graphic recorder he looks at edge alignment, length, and structural highlights. Analysis of these parameters can often reveal conclusively the presence or absence

of a submarine target. Generally, however, any single parameter is insufficient, and one expects the reliability of the classification to improve as more parameters are brought in.

It would be difficult to establish exactly how a given operator mentally processes such information to arrive at the contact classification. Even when they are presented identical data, two observers reach their respective decisions in somewhat different ways; for example, each may express a substantially different level of confidence in his response or even a different conclusion. Subjectivity is reduced when the decision process is performed rigidly and uniformly in all cases. NEL's Flexchart system, HHIP and MITEC were developed as aids to a uniform classification process. Established principles of decision theory can also be applied.

By assigning a numerical value, v_i, to each of the several measured parameters, p_i (display outputs), it is possible to write a general expression of the mathematical probability that a contact is a submarine. Suppose, as is depicted in figure 6, the prior probability of a contact's being a submarine (that proportion of the contact space which is submarines) is known. The shaded portion of the figure represents all those contacts in the space which display output values $v_1, v_2, \ldots, v_n$ or as a set V. Note that some are submarine contacts and some are non-submarine. The probability that a contact is a submarine is derived directly from the definition of a conditional probability and is often referred to as the inverse (or Baye's) probability law,

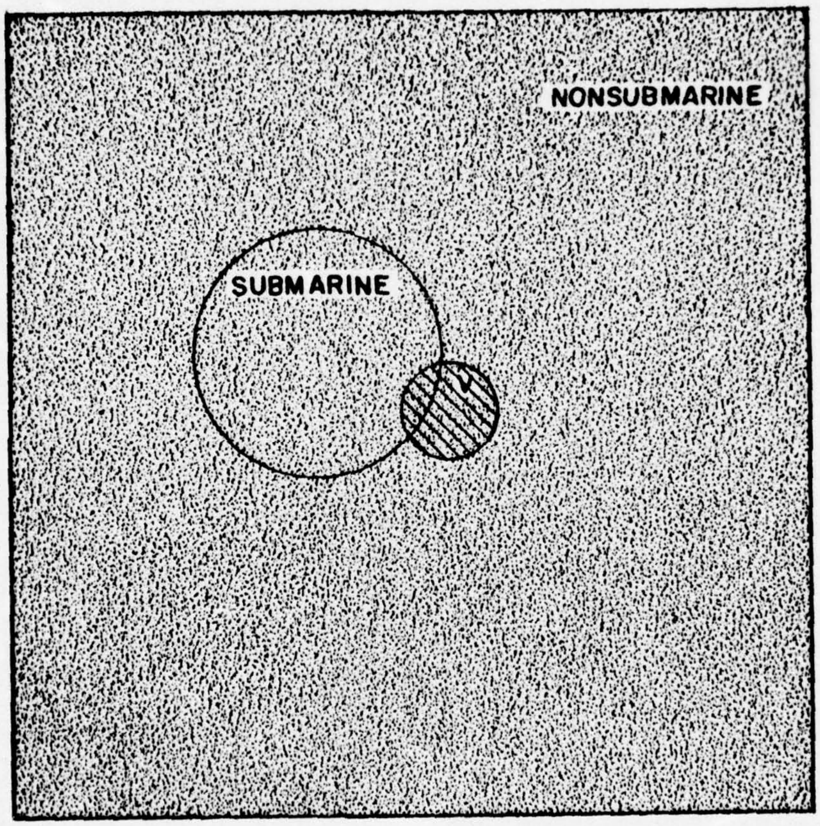

Figure 6. Contact Space

$$P(s|v_1, v_2, \ldots, v_n) = \frac{P(s)\ P(v_1, v_2, \ldots, v_n|s)}{P(v_1, v_2, \ldots, v_n)} \qquad (23)$$

which reads, "..... the probability that the contact is submarine; given that the value of parameter p_1 is v_1, p_2 is v_2," etc.

If the variables, v_i, range over a continuum of values, $P(s|v_1, v_2, \ldots, v_n)$ becomes a probability density function. The operator provided with the prior probability density functions $P(s)$, $P(v_1, v_2, \ldots, v_n|s)$ and $P(v_1, v_2, \ldots, v_n)$ could, at least in principle, compute the probability that a particular contact of measured parameters $(v_1, v_2, \ldots, v_n)$ is a submarine. Assuming a good selection of parameters, his average performance depends, of course, upon how well the prior probabilities represent the current situation. In the more practical approach, the sonarman depends upon his experience and training to provide this information.

A data processing system could be built to perform the computations of equation (23), aiding or, possibly, replacing the sonar operator in this function. This system, an inverse probability computer, provides storage for the functions (or their approximations) on the right-hand side of the equation. The reader familiar with the TRESI system will immediately note its similarity to an inverse probability computer.

In general, the conditioned-reflex (CR) concept represents a similar attack on the automatic classification problem; however, closer inspection reveals two important differences. First, it is oftentimes not known a priori which parameters should be

measured to permit reliable discrimination between several signal classes. One can suggest hundreds of possible sonar signal measurements that have been of value to contact classification; e.g., doppler, doppler derivative, echo length, envelope rise time, even sample levels themselves, etc. In the TRESI system, a restricted number of parameters have been selected and special instrumentation provided to measure each parameter. In the CR system, on the other hand, a large number (as many as 5000 in CONFLEX I) of linear threshold measurements generate parametric data to be used in the classification process. These measurements are relatively simple to implement and are all accomplished by essentially identical instrumentation. An important feature of this approach is the fact that the measurements are made without involvement of a human operator.

The second difference between the conventional inverse probability computer and the CR classification system is that, in the latter, cross-correlation is used as the basic decision function. As is well known, the correlation and inverse probability approaches are equivalent (with respect to a given set of parameters) when signal corruption is in the form of additive Gaussian noise, which, it is emphasized, is not the case in the sonar environment. The important advantage of cross-correlation is that relatively simple hardware is required for implementation of the computational algorithms. This is generally not true of the inverse probability computer.

SECTION III

DATA PREPARATION

As mentioned previously, experimental work with the CONFLEX I system requires that information to be classified be represented by a light transmission pattern on photographic slides. The data provided for the sonar classification experiments consisted of analog waveforms recorded on magnetic tape. Hence, the conversion to photographic patterns involved certain preprocessing of the signal data.

Signal preprocessing and slide preparation were greatly aided by the help of personnel from the Applied Mathematics Laboratory of the David Taylor Model Basin and the availability for this study of their analog-to-digital equipment, the IBM 7090 Computing System, and the GD/Stromberg-Carlson 4020 Microfilm Recorder. Program funding had been apportioned by the Bureau of Ships to the Model Basin for this assistance.

The sonar signal recordings included examples of both submarine and nonsubmarine returns. The recordings were contained on six reels of quarter-inch tape - four of which were chosen for the classification experiment. The data was obtained from the tape library of the Sonar Tape Analysis and Recording Department at the U. S. Fleet Anti-Submarine Warfare School, San Diego, California. Descriptive information relating to the reflectors accompanied the data.

Before digitizing the data, it was necessary to record on a second channel of the tape a negative trigger gate which was used by the analog-to-digital converter to initiate the sampling of each return. Localization of the echoes was accomplished by an experienced operator from an A-scope and audio display. Some 1514 returns were prepared in this manner; 17 examples of submarines (1153 returns) and 6 examples of nonsubmarines (361 returns).

Figure 7 illustrates the several steps involved in preprocessing the sonar signals. As shown in the figure, the sonar data was amplified, demodulated, and passed through a 300 cps low-pass filter. It was originally intended that demodulation and filtering would be performed after digitizing, but it was discovered that a disproportionate amount of computer time would be required. Design of a suitable detector and low-pass filter by SCOPE reduced the computer processing time per return from seven minutes to less than one minute, a large portion of which was required to produce an output format digital magnetic tape for the microfilm recorder. The raw sonar data and a demodulated and filtered return are shown in photographs (1) and (2) of figure 8.

Conversion of this waveform to digital form was accomplished using a ten bit analog-to-digital converter which began sampling on command from the analog recorder and continued until 1400 samples (700 msec) were generated. A plot of these samples is shown in photograph (3) of figure 8. These samples were recorded on digital magnetic tape and were subsequently read into the IBM 7090 computing system for further processing. The computer was

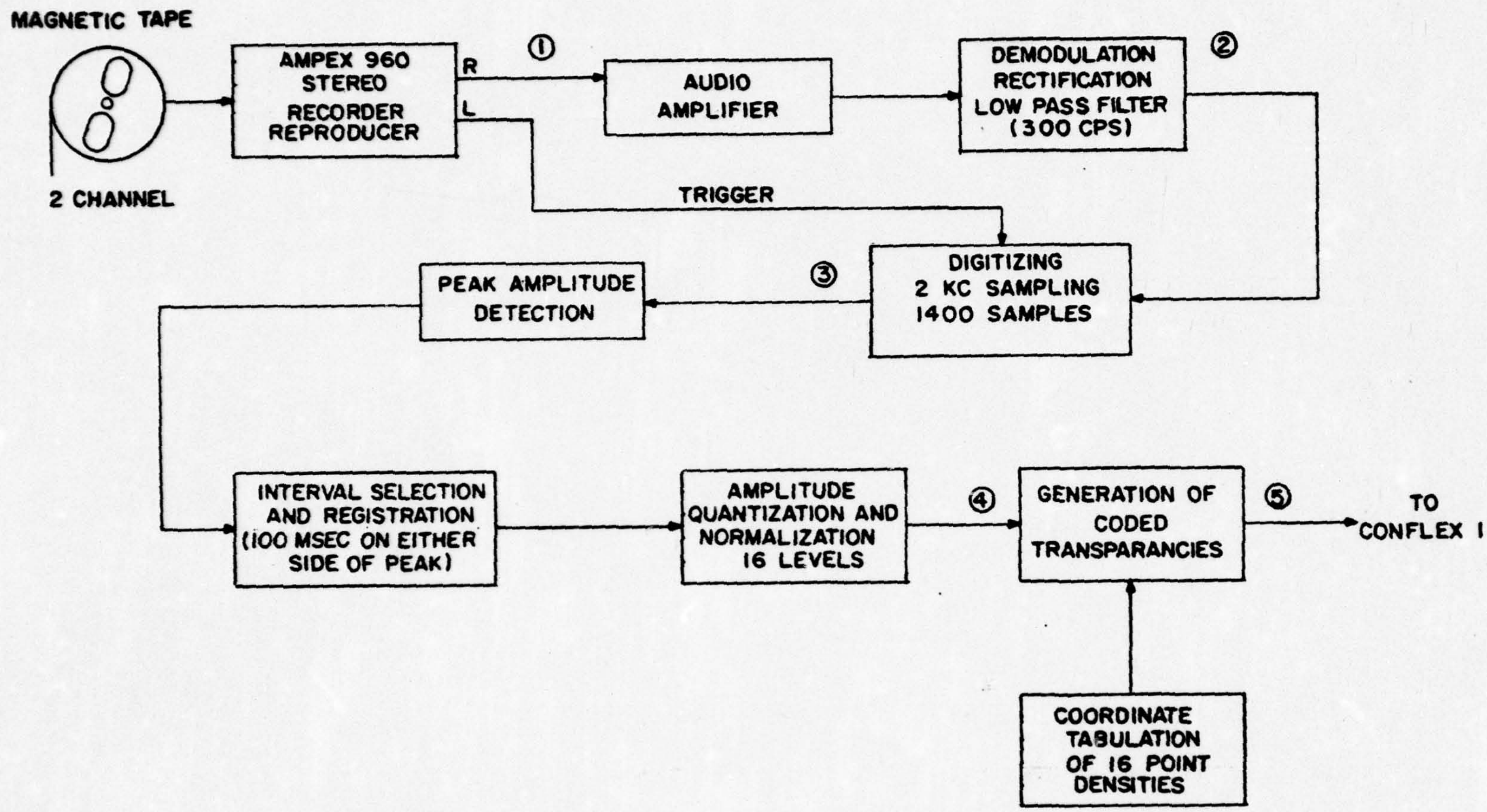

Figure 7. Functional Flow Diagram of the Submarine Return Preprocessing

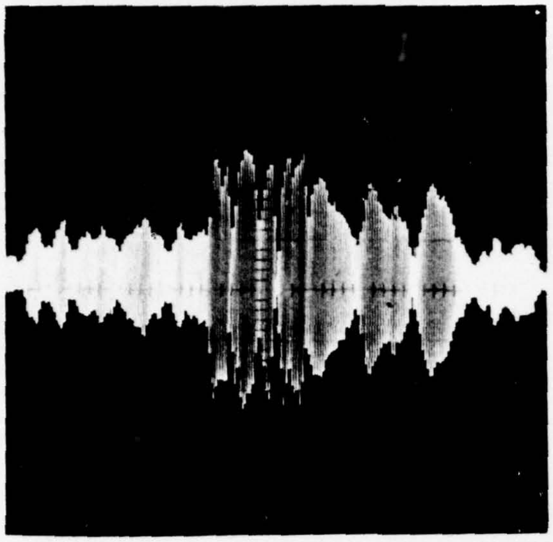

(1) Oscilloscope Photograph of Raw Data

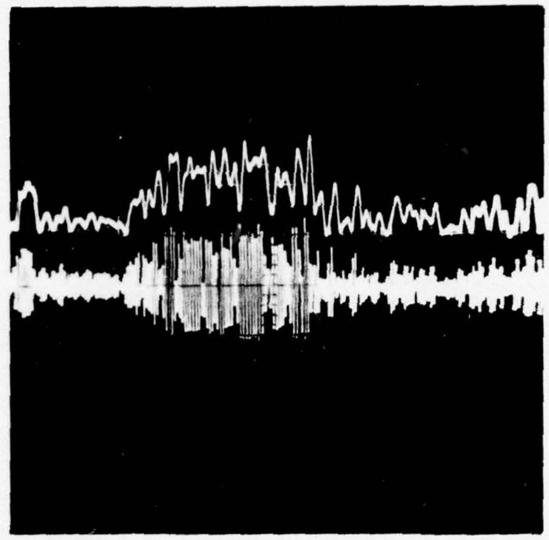

(2) Demodulated - Filtered Waveform and Raw Data From Which It Was Derived*

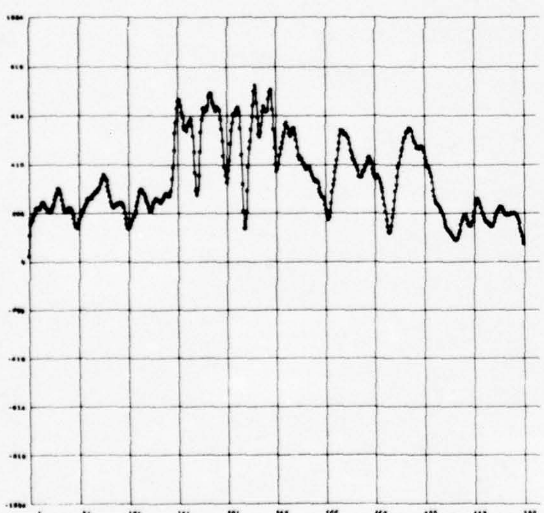

(3) Plot Taken From Digitized Data

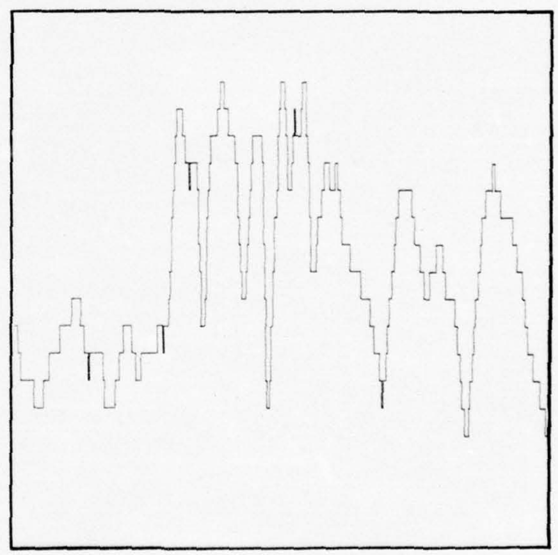

(4) Data Normalized And Quantized in 16 Amplitude Levels

*This waveform was taken from a different return from others on this page.

Figure 8. Illustrations of Preprocessing Stages

used to select 200 msec of the signal from the 700 msec originally sampled. The particular 200 msec selected corresponded to 100 msec on either side of the signal peak amplitude. Next, the computer normalized the data and requantized the 400 samples into 16 amplitude levels. The result of this operation is shown in photograph (4) of figure 8. Sixteen levels were chosen so as to correspond to the number of shades of gray that were developed for pattern representation in slide form. Coordinate data (36 points per amplitude level; a maximum of 576 points per sample) plus supporting format control data were then placed on magnetic tape for use by the SC 4020 microfilm recorder. The format for the patterns was generated as a separate computer subroutine. The several levels of gray on the microfilm were obtained by assigning a uniform point density linearly proportional to a corresponding signal amplitude. The progression of point densities from light to dark (corresponding to movement from low amplitude level to high amplitude level) was also linear. The film field was divided into 400 cells, each with a point density corresponding to the amplitude level of the signal sample to which that cell was assigned. Cell assignment remained fixed for all slides and, for the sake of convenience, was left-to-right, top-to-bottom.

The SC 4020 microfilm recorder under program control plots on its charactron tube any of 68 characters at any of 2^{20} plotting positions in a square matrix, then photographs the tube automatically at speeds up to seven frames per second. The processed 35 mm microfilm (a litho high-contrast) can also be used to generate xerographic hard copy of data which, with proper programming, can be produced in graphic or tabular form. If

point-density plots are used, the coded photographic transparencies are formed in much the same fashion as half-tone prints.

The resulting slide for the waveform shown in figure 8(1) is reproduced in figure 9. It will be noticed that the pattern is divided into 400 squares or cells, one per sensor input to CONFLEX I and each corresponding to an amplitude sample of the waveform envelope.

The SC 4020 microfilm recorder is currently operated at DTMB as an off-line equipment and must therefore take its input from digital magnetic tape. A very large number of plotting coordinates (approximately 120,000 on the average), in addition to format control, had to be read in to generate a single slide. This resulted in an unexpectedly long time (about 45 seconds) to generate the pattern and of course increased the cost per slide to an unrealistic level. The original cost estimate was less than ten cents per frame, conservatively based upon the speed quotation previously mentioned (7 frames/second). We have since discovered that the originally stated specifications apply to an on-line system.

We therefore felt it unwise to continue to generate transparencies at this high cost in view of the size of the data set. Our search for a more realistic input buffer led us to propose a more complex but far more efficient and flexible system. We are pleased that construction of the system, which utilizes an SDS-925 general-purpose computer in direct electrical communication with the CONFLEX I was funded under BUSHIPS Contract NObsr

7	7	7	7	6	6	5	5	5	5	5	5	5	5	5	5	4	4	4	4
4	4	4	5	5	5	5	6	6	6	6	6	6	6	6	7	7	7	7	7
7	7	7	8	8	8	8	8	8	8	7	7	7	6	6	6	5	6	6	6
6	6	6	6	6	6	6	5	4	4	4	4	4	4	4	4	5	5	5	6
6	6	7	7	7	7	7	7	6	6	6	5	5	5	5	6	6	6	6	6
6	6	6	6	6	6	6	7	7	7	7	6	7	7	7	8	9	v	w	x
y	z	z	z	z	y	y	x	x	x	w	x	x	x	x	x	w	u	9	7
7	7	8	v	w	x	y	y	y	y	y	z	z	m	m	m	z	z	z	y
y	y	y	y	x	x	v	u	9	8	8	8	9	u	v	w	x	y	y	y
y	y	y	y	x	u	8	5	4	4	5	7	9	v	v	w	y	z	m	m
m	z	y	w	w	w	x	y	z	y	y	y	y	z	m	m	m	y	x	v
9	9	9	9	u	v	v	v	w	w	x	x	x	x	w	w	w	w	x	x
w	w	v	u	u	u	u	u	u	9	9	9	9	9	9	9	9	8	8	8
8	8	8	8	7	7	7	6	6	6	6	5	5	4	5	5	6	7	8	8
9	9	u	v	v	w	w	w	w	w	w	w	w	w	w	v	v	u	u	u
u	9	9	9	8	8	8	8	9	9	9	9	9	u	u	u	u	u	9	9
8	8	8	8	8	8	8	7	7	6	6	5	4	4	3	3	3	4	5	5
6	7	8	8	9	9	u	v	v	v	w	w	w	w	w	x	x	w	w	w
w	v	v	v	v	v	v	v	v	v	u	u	u	9	9	9	9	8	8	7
7	6	6	6	6	5	5	5	5	5	4	4	4	4	3	3	3	3	3	3

Amplitude Levels for Coded Transparency of Figure 9
(u thru z and m represent 10 thru 15 and 16, respectively.)

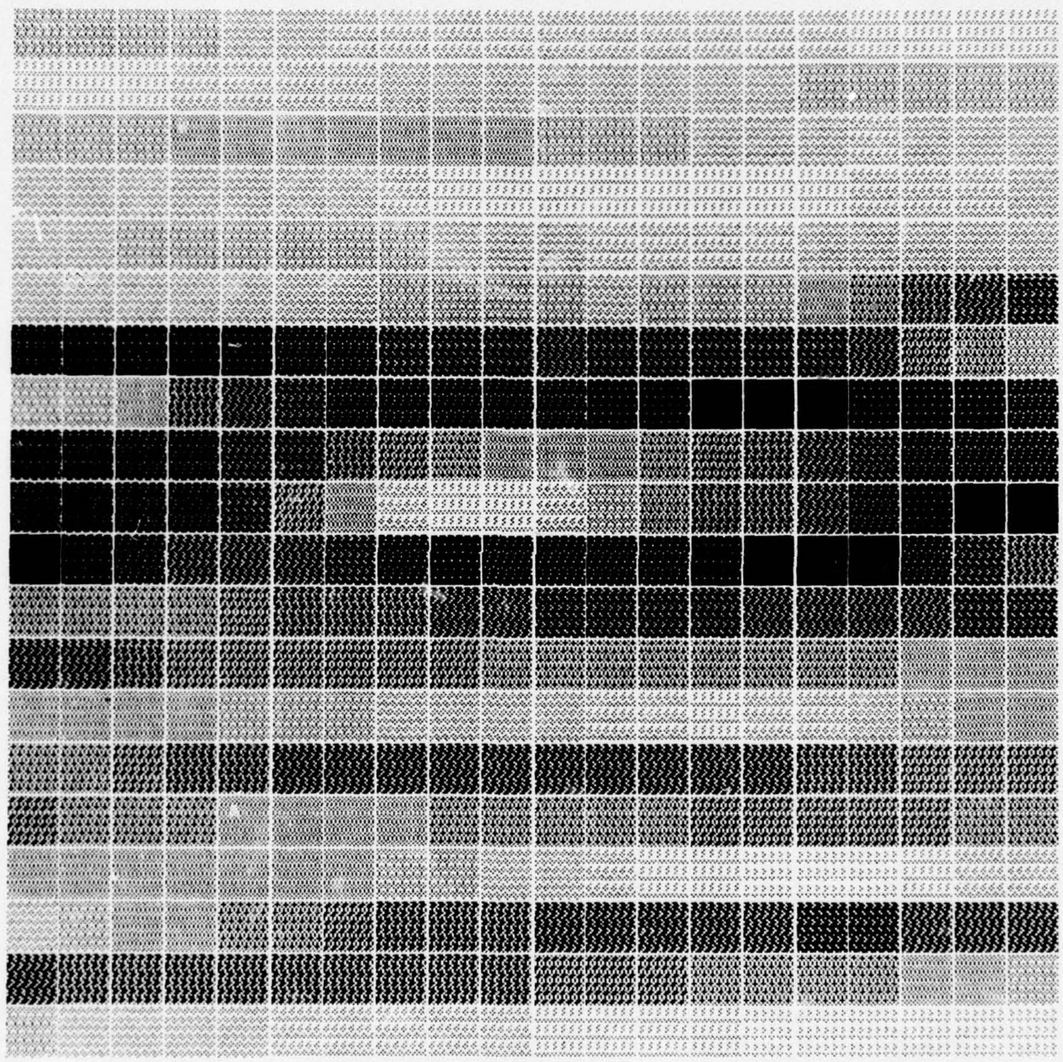

Figure 9. Coded Photographic Transparency Representing Sonar Return

93231 and is now operating. This increased efficiency was particularly necessary due to an order of magnitude increase in the data set.

Nevertheless, SCOPE was directed to continue the program, using the SC 4020 to generate slides on as much of the data as remaining funds allowed. This data was then to serve as the data base for the classification experiments. Included in this set were 205 returns, 132 returns from a single submarine example and 73 returns from three nonsubmarine examples. The submarine was described in the accompanying legend as a beam-to-bow aspect submarine showing secondary echoes. The nonsubmarine examples were described as biologics and fishnets; a single, large biologic; and kelp patches with good audio qualities and with no change in length. The type of sonar and its frequency and mode were not given, however, we believe it to be an SQS-4 series sonar in medium pulse mode. Results of experiments with these inputs are contained in Section IV.

SECTION IV

EXPERIMENTS

The experiments performed during this study were designed to evaluate the capability of the CONFLEX I pattern recognition system to distinguish representations of a number of sonar returns of submarine reflectors from those of nonsubmarine reflectors. The particular data set consisted of 205 returns, 132 returns from a single submarine example and 73 returns from three nonsubmarine examples. As mentioned previously, the submarine reflector was described in the legend that accompanied it as a beam-to-bow aspect submarine showing secondary echoes. The nonsubmarine examples were likewise described as biologics and fishnets; a single, large biologic; and kelp patches with good audio qualities and with no change in length. The data provided for these experiments consisted of the audio display output recorded on magnetic tapes. Preprocessing and formating have been detailed previously in Section III.

Three major experiments involving the submarine and nonsubmarine returns were run on the CONFLEX I. The first consisted of training the system with all submarine returns in class S and all nonsubmarine returns in class NS. To test the system's ability to separate these two classes in this "closed end" (no unknowns) case, all inputs were then applied and the resulting class assignments and correlations with the reference functions were recorded.

In the second experiment, to obtain a measure of the system's ability to categorize inputs which had not been used for training (the "open-ended case"), a set of 66 (the odd-numbered submarine) returns from each of classes S and NS was selected for the conditioning process. The "unknown" inputs were then applied for class assignment. Error correction procedures were also explored. To test the performance of CONFLEX I when the submarine return population was subdivided into several classes according to aspect, a third experiment was performed. Six aspect classes were defined in the training routine. The nonsubmarine population was subdivided into three classes according to the type of contact.

CLOSED END EXPERIMENT

Of the 132 returns in the S class, one submarine return was misclassified and one assignment was a borderline case for a correct S classification rate of 98.5%. (The borderline case was counted as an error.) Four of the 73 nonsubmarine returns were misclassified and ten were borderline decisions. Counting half of the borderline cases as correct (corresponding to chance selection), nonsubmarine returns were correctly classified at a rate of 87.7%. The total correct classification rate for the entire input was 94.1%.

Figure 10 is a distribution plot of the correlation values obtained when all inputs (both submarine and nonsubmarine returns) were compared with the S class reference function. If a threshold level is set at 640 and all inputs which evoked a larger

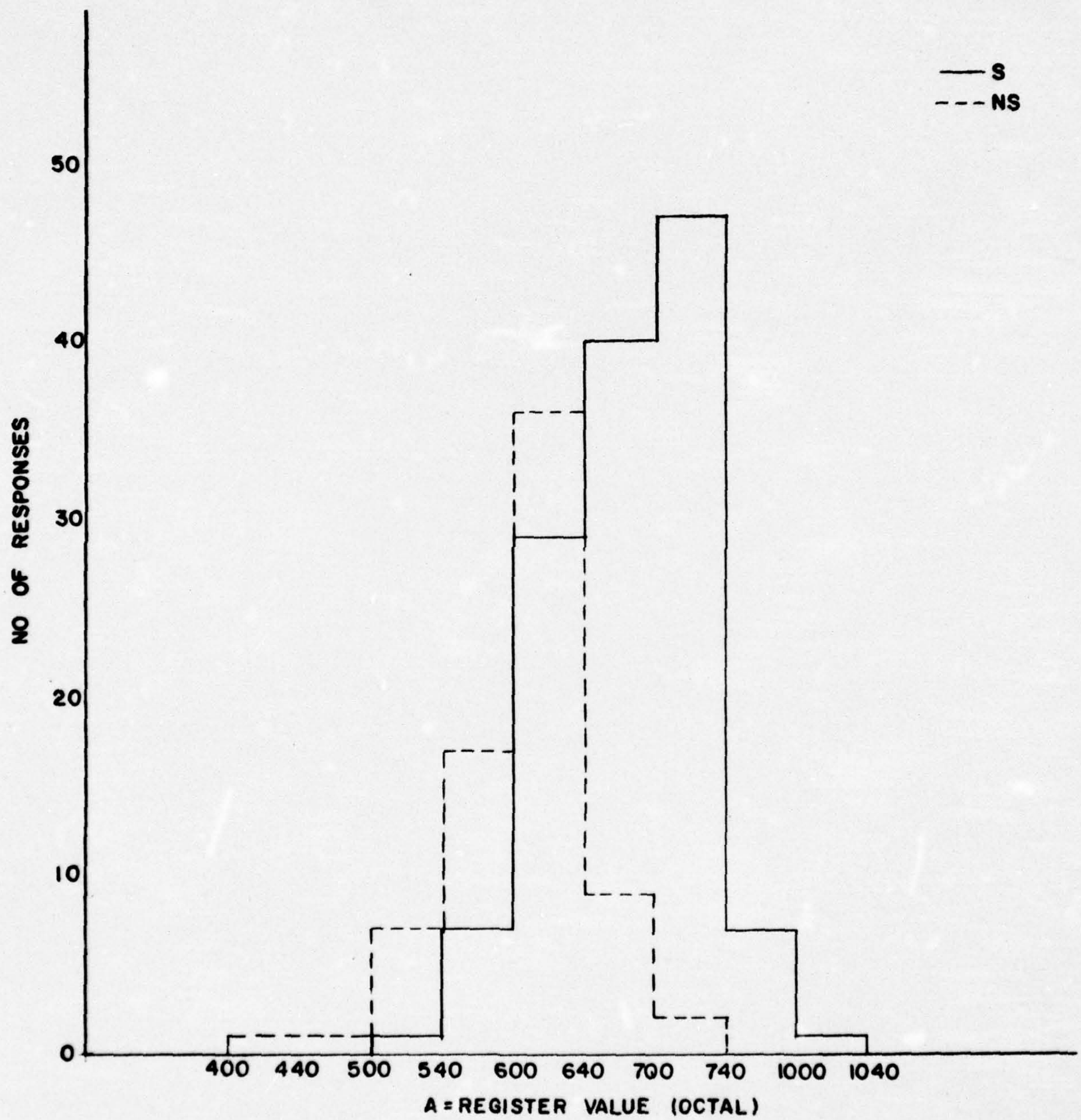

Figure 10. Distribution of Correlation Values with S Reference Function

correlation value are called submarine and those inputs with lower correlation values nonsubmarine, a correct classification rate for the submarine returns of 72.0% is observed. The non-submarine return inputs yield 84.9% correct response. A lower threshold setting at 600 yields a 93.9% correct classification rate for the submarine returns and 35.6% for the nonsubmarine inputs. Note that these results are achieved with training utilizing only submarine returns. A similar distribution is plotted for the correlation values obtained when all inputs were compared with the NS class reference function. With a threshold setting of 640, a correct submarine classification rate of 87.9% is obtained and 39.7% for the nonsubmarine returns.

Curves can be derived from each of the above two distributions which characterize the system performance (often referred to as "ROC," receiver operating characteristic, curves) when a comparison of the correlation value with a fixed threshold is used as the decision criteria. The threshold setting becomes a parameter. Two types of errors are defined: "error 1" occurs when the input is called a member of class NS when, in fact, it is a member of class S; "error 2" occurs when the input is called a member of class S when, in fact, it is a member of the NS category. Figures 12 and 13 are the "ROC" curves generated from the distributions shown in figures 10 and 11, respectively. The chance line always shows an equal total number of errors. Notice that the "best case" in each of the figures is 77% and 78% correct response, respectively. This is somewhat less than the 94% correct classification rate achieved by CONFLEX I, because CONFLEX I uses a correlation value comparator for its assignment criteria rather than the fixed threshold.

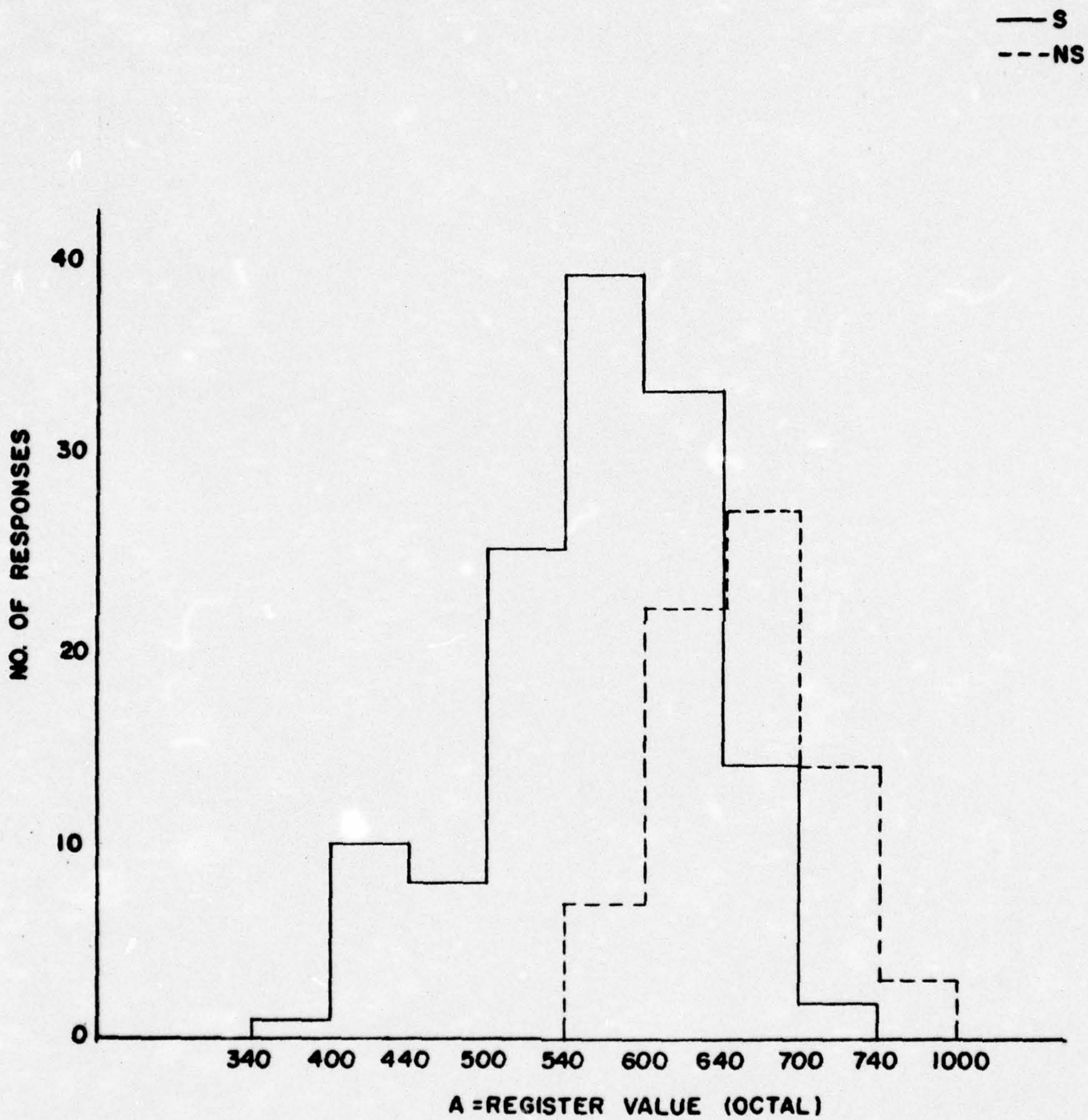

Figure 11. Distribution of Correlation Values with NS Reference Function

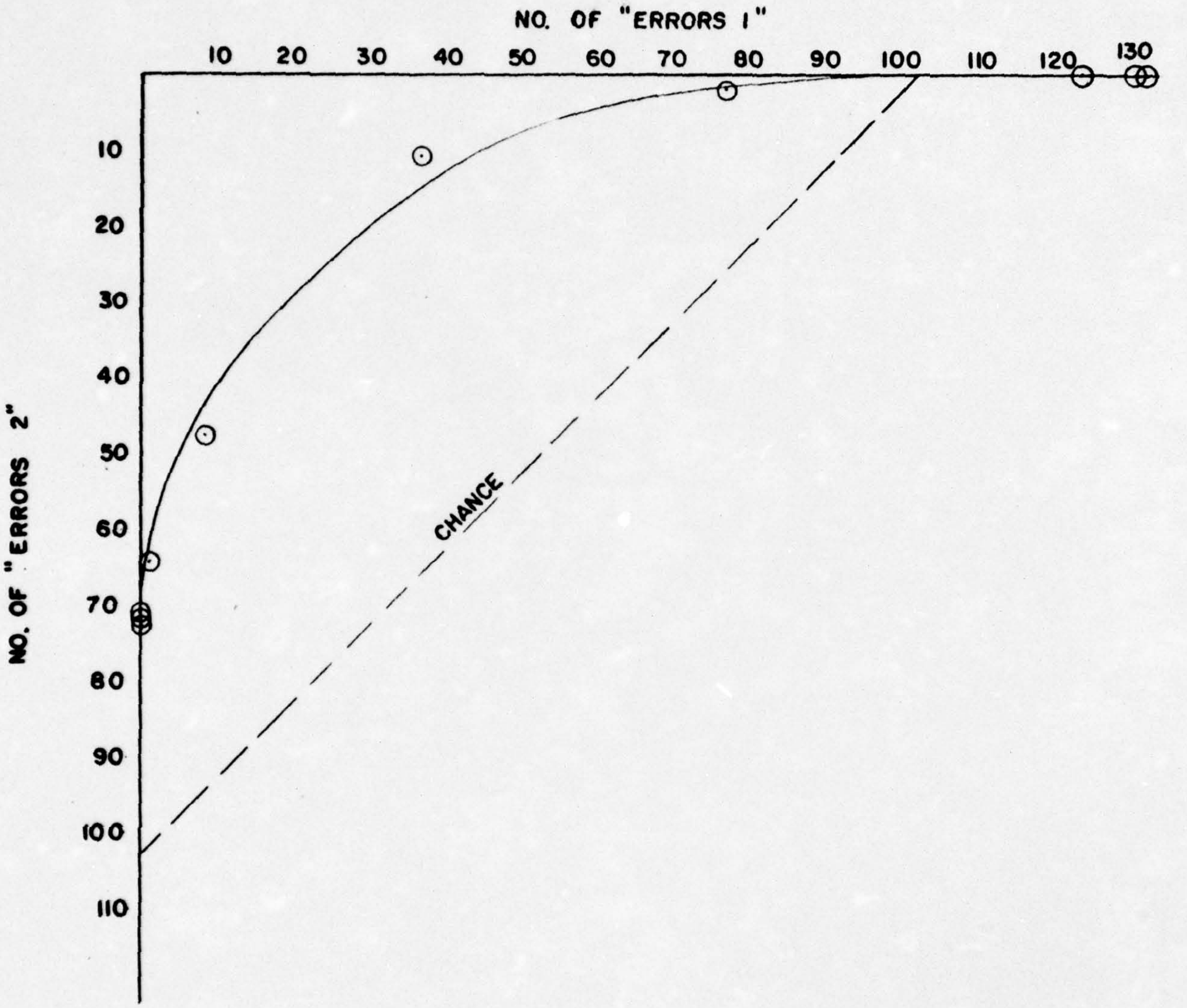

Figure 12. "ROC" Curve for Distribution of Figure 10

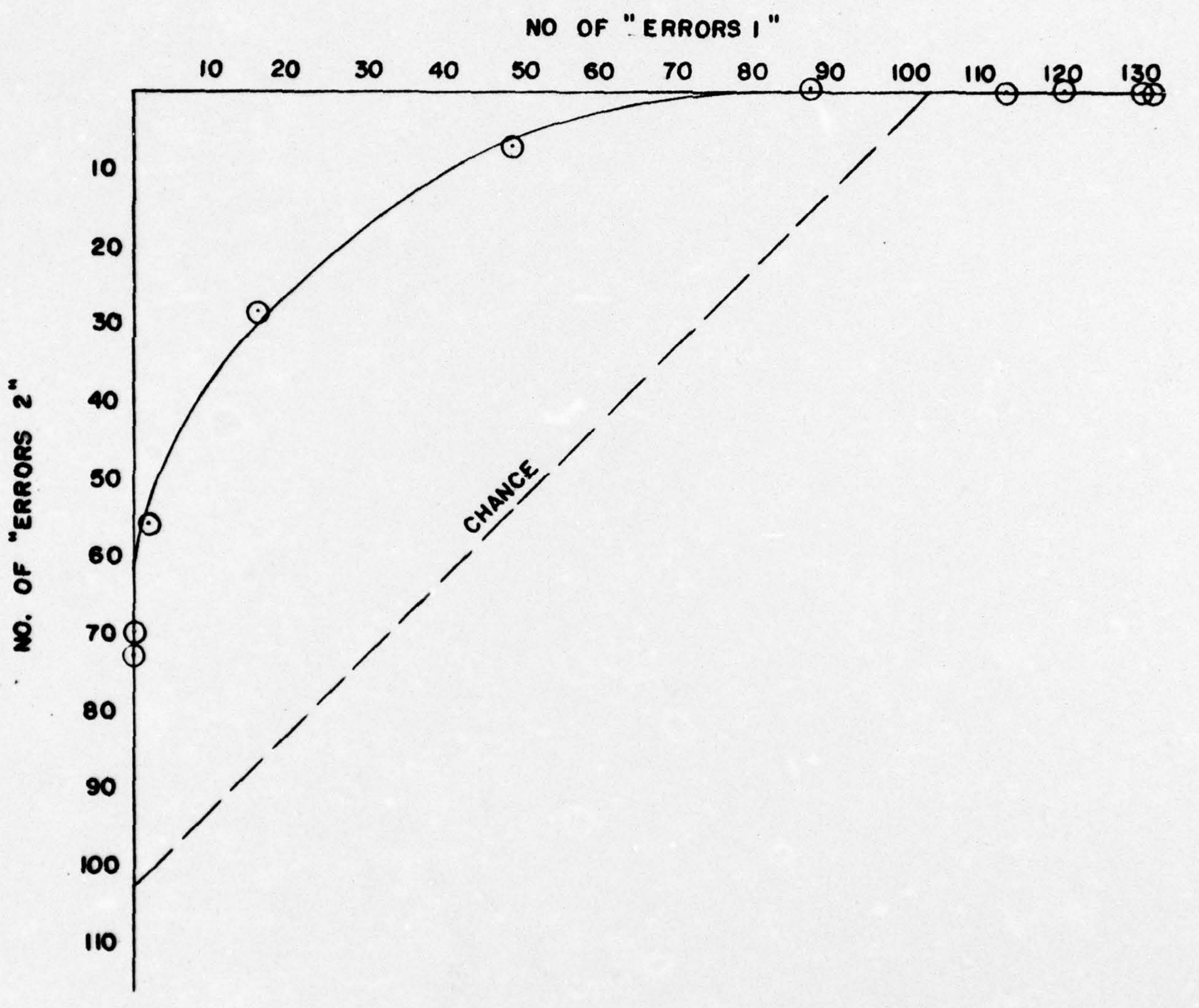

Figure 13. "ROC" Curve for Distribution of Figure 11

Using the in-class and out-of-class correlation values obtained in this experiment, we find that

$\mu_S = 431 \equiv$ mean of the in-class values

$\mu_N = 373 \equiv$ mean of the out-of-class values

$\sigma_S^2 = 1028 \equiv$ variance of the in-class values

$\sigma_N^2 = 1783 \equiv$ variance of the out-of-class values

Cov = 447 $\equiv$ covariance of the in-class and out-of-class values

An experimental Γ may be computed by substituting these values into the expression for Γ (equation 19, Section I),

$$\Gamma = \frac{(\mu_S - \mu_N)}{\sigma_T} = \frac{(\mu_S - \mu_N)}{\sqrt{\sigma_S^2 + \sigma_N^2 - 2\ \mathrm{Cov}}} = \frac{431 - 373}{\sqrt{1028 + 1783 - 2(447)}}$$

$$\Gamma = 1.3$$

As noted in the appendix, a Γ of 1.3 indicates a probability of correct response equal to 0.9032 or an expected error rate of 968 per 10,000 in a two-class experiment. This compares with a correct response rate of 0.941 for the data set.

OPEN END EXPERIMENT

Of the 66 submarine returns used in training the S class, seven were misclassified as NS and one decision was borderline for a correct S classification rate of 87.9%. (The borderline case counted as an error.) Of the 66 unknown submarine returns (those not used in training), 72.7% were correctly classified. Two of the 66 nonsubmarine returns used in training were called S, and one assignment was borderline for a correct classification rate of 95.5%. (The borderline case again counted as an error.) Six of the seven unknown nonsubmarine returns were correctly called NS. Classification of the entire set of submarine returns was 80.3% correct, even though half (every other one) of these returns were not used in the training. Overall NS classification was 94.5% correct. Error correction procedures improved these responses to 89.4% and 95.9%, respectively.

MULTICLASS EXPERIMENT WITH ASPECT ANGLE GROUPING

As mentioned previously, a change in the target angle, hence echo length, of the reflector is one variation among several which serve to reduce the singularity of the class reference sequence and thus degrade the performance of the classification system. The submarine example in the data set was described as a "beam-to-bow aspect submarine." It would seem that the results of experiment 1 could have been improved by conditioning the processor with several groups of the submarine returns arranged according to increments of target angle rather than a full range of aspects in one class. This was the case.

In experiment 3, six aspect groups were defined using equal 18 degree increments beam to bow as depicted in figure 14 by training equal groups of 22 returns each, first to last. The assumption of course, is that the submarine's rate of change of target angle was linear with respect to the ping rate. We have no data describing the submarine's aspect during the run other than that given above. The nonsubmarine returns were also subdivided into three classes according to the type of contact.

All but two of the submarine returns were classified as one of the six submarine groups for a correct classification rate of 98.5%. All but three of the nonsubmarine returns were placed in one of the NS categories for a correct nonsubmarine classification of 95.9%. Response for the entire data set was 97.6% correct.

Individual aspect group responses were 90.9%, 90.9%, 95.4%, 86.4% 86.4% and 90.9% correct progressing from bow to beam. Individual nonsubmarine class responses were 91.3%, 96.0%, and 72.0% correct for the biologics and fishnets; the single large biologic; and the kelp patches, respectively. Of the submarine returns, 91.7% were associated with the correct aspect class; of the nonsubmarine returns, 88.4% were associated with the correct nonsubmarine example.

The borderline cases (those inputs which evoke nearly the same highest correlation with more than one class) always included the correct aspect group or nonsubmarine example as one of the choices. The other choice was always another aspect group

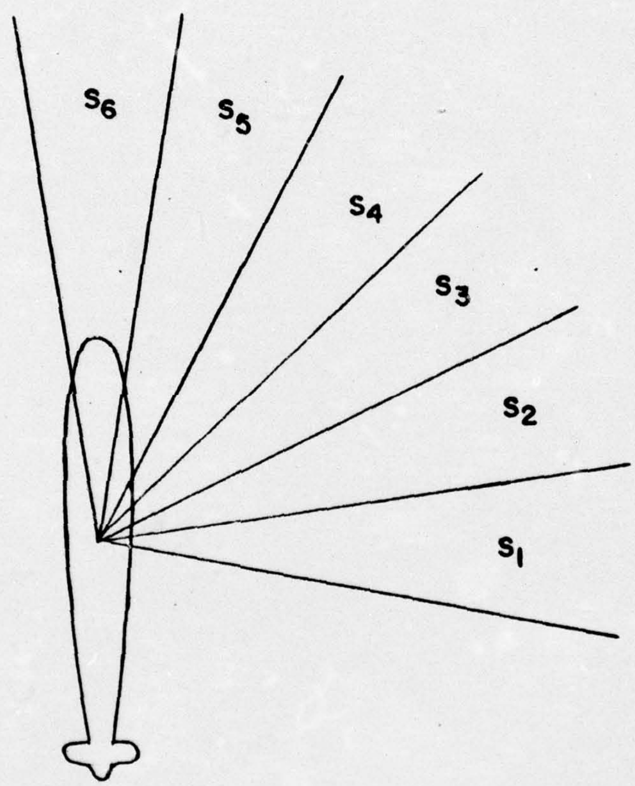

Figure 14. Aspect Groupings for Experiment 3

in the submarine case and another nonsubmarine example in two of three nonsubmarine example borderline cases. Half (4) of the other aspect group choices were an adjoining aspect group to the correct class.

Five of the seven submarine return incorrect aspect group classifications were still submarine classifications. Two of these were classifications as an adjoining aspect group to the correct group. Four of the seven nonsubmarine return misclassifications were instead associated with another nonsubmarine example. The second choice (second highest correlation value) for the seven submarine return incorrect aspect group classifications was in all cases another submarine aspect group, four times the correct submarine aspect group and once of the other three an adjoining aspect group. The second choice for the seven nonsubmarine return incorrect example classifications was in five cases nonsubmarine example, four of which were the correct example.

In the cases (117) of correct submarine return aspect group classifications, the next highest correlation value was another submarine aspect group 113 times, an adjoining submarine aspect group 59 times and a nonsubmarine example only four times.

Figures 15 through 19 are distribution plots of the correlation values obtained when all submarine return inputs were compared with the first submarine aspect group. Each figure shows the distribution plot for a different aspect group. Correspondingly, figure 20 is a composite plot of the "ROC" curves for these distributions. The two errors in these cases are defined:

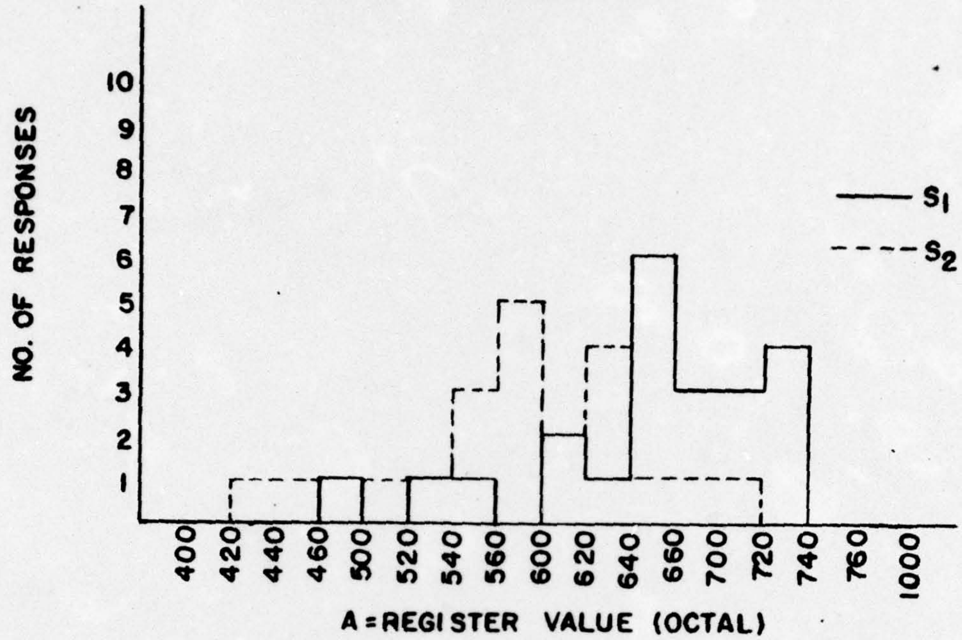

Figure 15. Distribution of S_1, S_2 Aspect Group Returns with S_1 Reference Functions

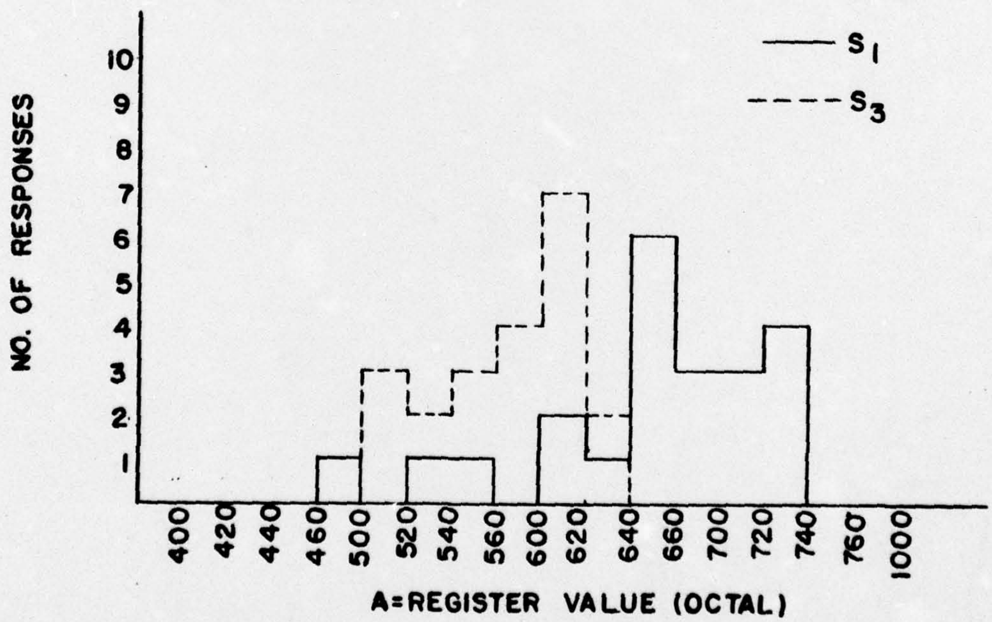

Figure 16. Distribution of S_1, S_3 Aspect Group Returns with S_1 Reference Functions

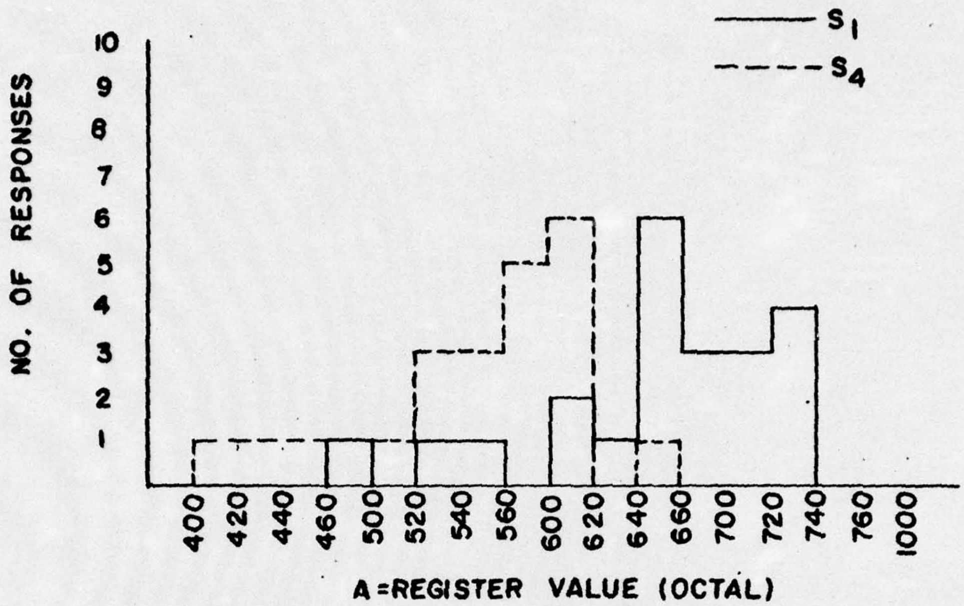

Figure 17. Distribution of S_1, S_4 Aspect Group Returns with S_1 Reference Function

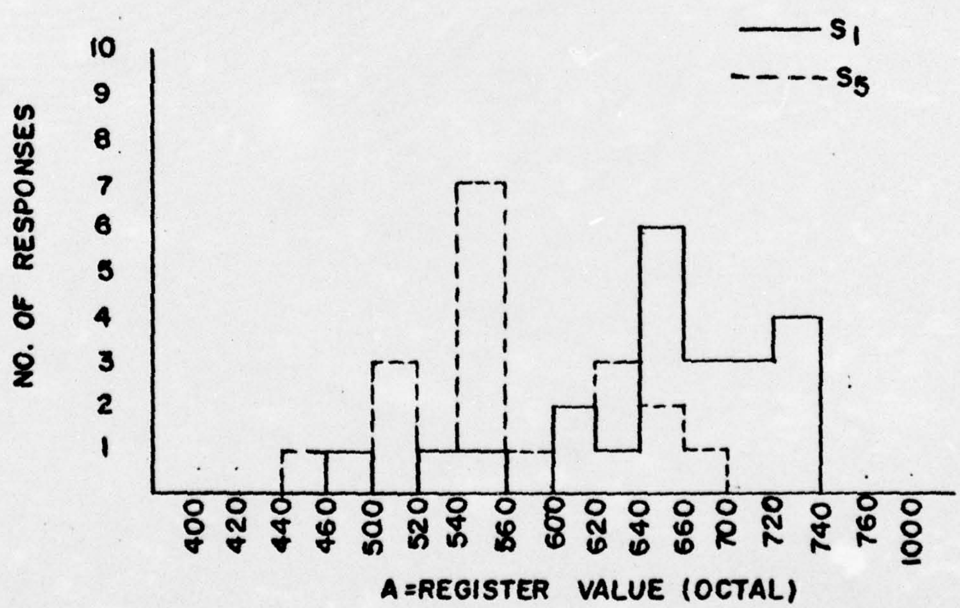

Figure 18. Distribution of S_1, S_5 Aspect Group Returns with S_1 Reference Function

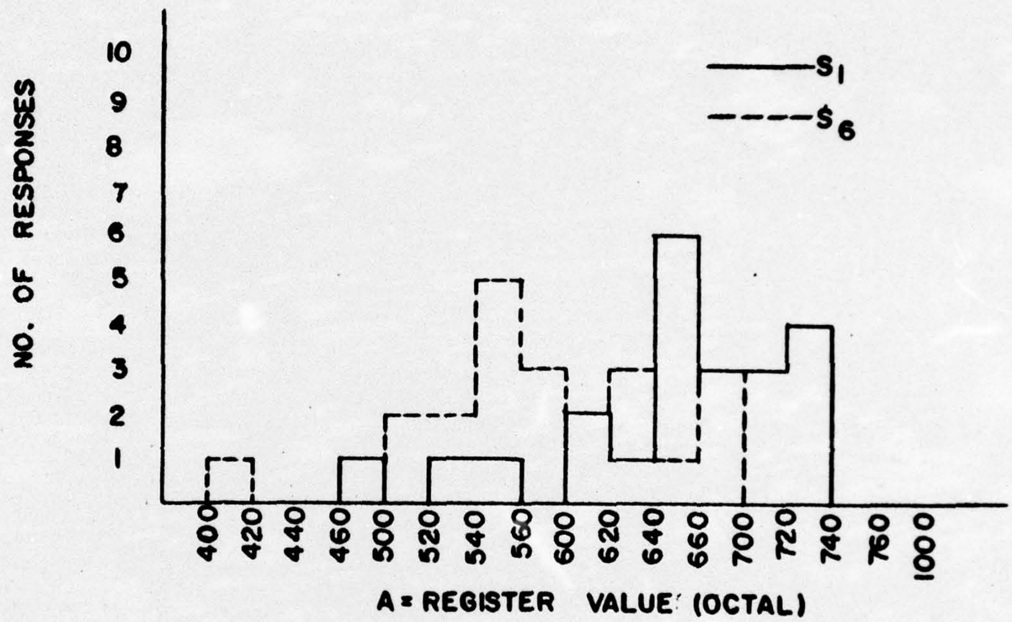

Figure 19. Distribution of S_1, S_6 Aspect Group Returns with S_1 Reference Function

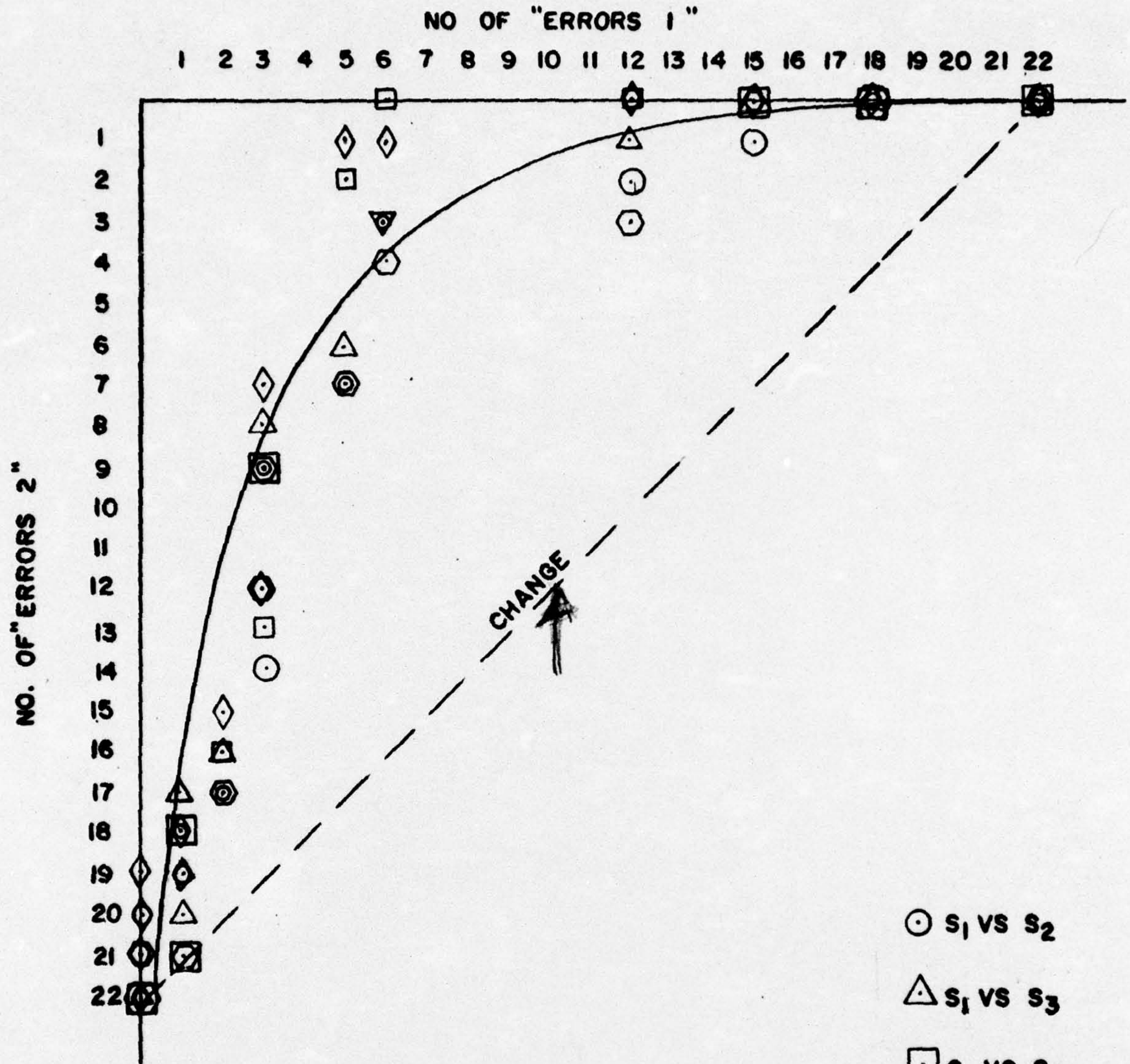

Figure 20. Composite Plot of "ROC" Curves for Figures 15-19

"error 1" occurs when the input is called a member of aspect group S_i (i = 2, 3 ... 6) when in fact it is a member of aspect group S_1; "error 2" occurs when the input is called a member of aspect group S_1 when in fact it is a member of aspect group S_i.

One final result from this experiment is plotted in figure 21. The upper curve is a plot of the percent change in calculated echo length (transmission pulse considered) as the submarine's aspect changes from beam to bow. The lower curve represents the percent decrease in the average correlation value of the returns from each of the aspect groups when compared with the S_1 reference function. The percent decrease of each aspect group's lowest correlation value is shown by the dotted curve. As expected the trend is downward in these latter curves, however at not nearly the rate of the change in pulse length. The dependence of pulse length upon performance is not evident from this set of curves.

14,500-c

CONFIDENTIAL

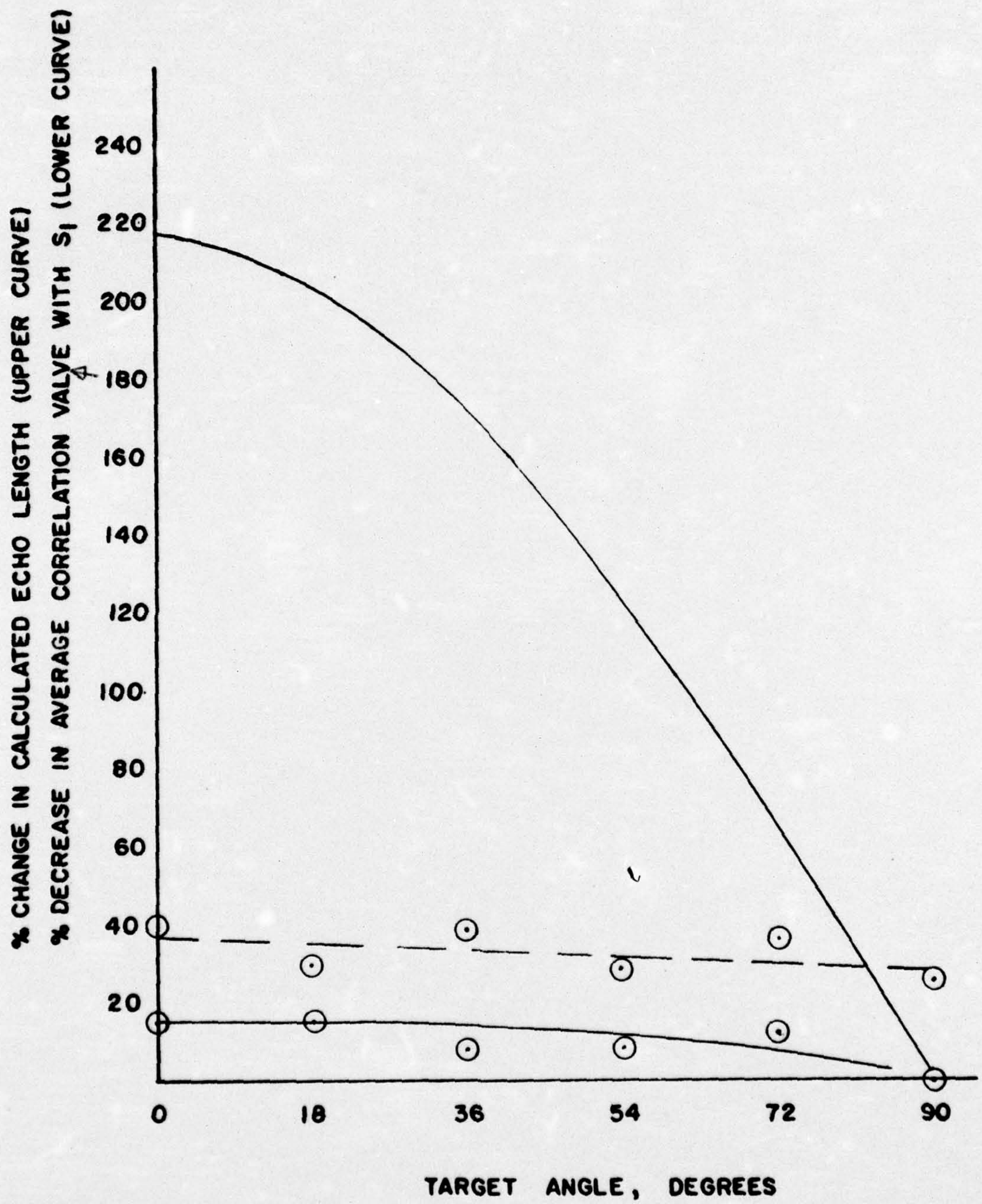

Figure 21. Comparison of Percent Change in Pulse Length with Aspect Angle and Percent Decrease in Correlation Value

14,500-C

REFERENCES

1. "Study of Automatic Conditioned-Reflex Jamming Mode Selector," Technical Documentary Report No. ASD-TDR-62-402, Contract No. AF33(616)-7268, SCOPE Incorporated, 30 March 1962.

2. R. S. Burington, "Handbook of Mathematical Tables and Formulas", 2nd Edition, Handbook Publishers, Inc., Sandusky, Ohio, 1947.

3. E. Parzen, "Modern Probability Theory and Its Applications," John Wiley and Sons, Inc., New York, 1960.

4. "Development of an Advanced Conditioned-Reflex Model," First Quarterly Progress Report, Contract No. AF33(657)-7509, SCOPE Incorporated, 20 February 1962.

[redacted]

UNCLASSIFIED

APPENDIX

TWO-CLASS PROBABILITY OF CORRECT RESPONSE AS A FUNCTION OF Γ

Γ	P'_c	Γ	P'_c
0.0	0.5000	2.0	0.9772
0.1	0.5398	2.1	0.9821
0.2	0.5793	2.2	0.9861
0.3	0.6179	2.3	0.9893
0.4	0.6554	2.4	0.9918
0.5	0.6915	2.5	0.9938
0.6	0.7257	2.6	0.9953
0.7	0.7580	2.7	0.9965
0.8	0.7881	2.8	0.9974
0.9	0.8159	2.9	0.9981
1.0	0.8413	3.0	0.9987
1.1	0.8643	3.1	0.9990
1.2	0.8849	3.2	0.9993
1.3	0.9032	3.3	0.9995
1.4	0.9192	3.4	0.9997
1.5	0.9332	3.5	0.9998
1.6	0.9452	3.6	0.9998
1.7	0.9554	3.7	0.9999
1.8	0.9641	3.8	0.9999
1.9	0.9713	3.9	1.0000

UNCLASSIFIED

[redacted]